Icarus 208 (2010) 636–657

Contents lists available at ScienceDirect

Icarus

journal homepage: www.elsevier.com/locate/icarus

Evidence for pervasive mud volcanism in Acidalia Planitia, Mars

Dorothy Z. Oehler *, Carlton C. Allen

Astromaterials Research and Exploration Science Directorate, NASA-Johnson Space Center, 2101 NASA Parkway, Houston, TX 77058, USA

ARTICLE INFO

Article history:
Received 29 August 2009
Revised 16 March 2010
Accepted 24 March 2010
Available online 1 April 2010

Keywords:
Mars, Surface
Astrobiology

ABSTRACT

We have mapped 18,000+ circular mounds in a portion of southern Acidalia Planitia using their sizes, shapes, and responses in Nighttime IR. We estimate that 40,000+ of these features could occur in the area, with a distribution generally corresponding to the southern half of the proposed Acidalia impact basin. The mounds have average diameters of about 1 km and relief up to 180 m and most overlie units mapped as Early Amazonian.

High resolution images of mound surfaces show relatively smooth veneers, apron-like extensions onto the plains, moats, and concentric circular crestal structures. Some images show lobate and flow-like features associated with the mounds. Albedo of the mounds is generally higher than that of the surrounding plains. Visible and near-infrared spectra suggest that the mounds and plains have subtle mineralogical differences, with the mounds having enhanced coatings or possibly greater quantities of crystalline ferric oxides.

Multiple analogs for these structures were assessed in light of new orbital data and regional mapping. Mud volcanism is the closest terrestrial analogy, though the process in Acidalia would have had distinctly martian attributes. This interpretation is supported by the geologic setting of the Acidalia which sits at the distal end of the Chryse–Acidalia embayment into which large quantities of sediments were deposited through the Hesperian outflow channels. In its distal position, Acidalia would have been a depocenter for accumulation of mud and fluids from outflow sedimentation.

Thus, the profusion of mounds in Acidalia is likely to be a consequence of this basin's unique geologic setting. Basinwide mud eruption may be attributable to overpressure (developed in response to rapid outflow deposition) perhaps aided by regional triggers for fluid expulsion related to events such as tectonic or hydrothermal pulses, destabilization of clathrates, or sublimation of a frozen body of water. Significant release of gas may have been involved, and the extensive mud volcanism could have created long-lived conduits for upwelling groundwaters, providing potential habitats for an *in situ* microbiota.

Mud volcanism transports minimally-altered materials from depth to the surface, and mud volcanoes in Acidalia, therefore, could provide access to samples from deep zones that would otherwise be inaccessible. Since the distal setting of Acidalia also would favor concentration and preservation of potentially-present organic materials, samples brought to the surface by mud volcanism could include biosignatures of possible past or even present life. Accordingly, the mounds of Acidalia may offer a new class of exploration target.

1. Introduction

The potential for mud volcanism in the Northern Plains of Mars has been recognized for some time, with candidate mud volcanoes reported from Utopia, Isidis, northern Borealis, Scandia, and the Chryse–Acidalia region (Davis and Tanaka, 1995; Tanaka, 1997, 2005; Tanaka et al., 2000, 2003, 2008; Farrand et al., 2005; Kite et al., 2007; Rodríguez et al., 2007; Skinner and Tanaka, 2007; Allen et al., 2009; Oehler and Allen, 2009; Skinner and Mazzini, 2009; McGowan, 2009; McGowan and McGill, 2010). We have focused on the mud volcano-like mounds in Acidalia Planitia (Figs. 1–3), as these features are present in enormous numbers and may reflect a major event in the history of the martian lowlands.

The Acidalia mounds (Figs. 2 and 3) were first noted in Viking imagery (Allen, 1979; Frey et al., 1979; Frey and Jarosewich, 1982) and have been variously interpreted as pseudocraters, cinder cones, tuff cones, pingos, or ice-disintegration features (summarized in Tanaka (1997), Tanaka et al. (2005), and Farrand et al. (2005)). Recently, they have been compared to mud volcanoes (Tanaka et al., 2003, 2005) or some combination of mud volcanoes and evaporite deposition around geysers and/or springs (Farrand et al., 2005). Our work uses new orbital data coupled with regional mapping and basin analysis to evaluate the distribution of the mounds as well as the details of their surface geomorphology. New images from the Context Camera (CTX) and High Resolution Imaging

* Corresponding author.
E-mail address: dorothy.z.oehler@nasa.gov (D.Z. Oehler).

0019-1035/$ - see front matter © 2010 Elsevier Inc. All rights reserved.
doi:10.1016/j.icarus.2010.03.031

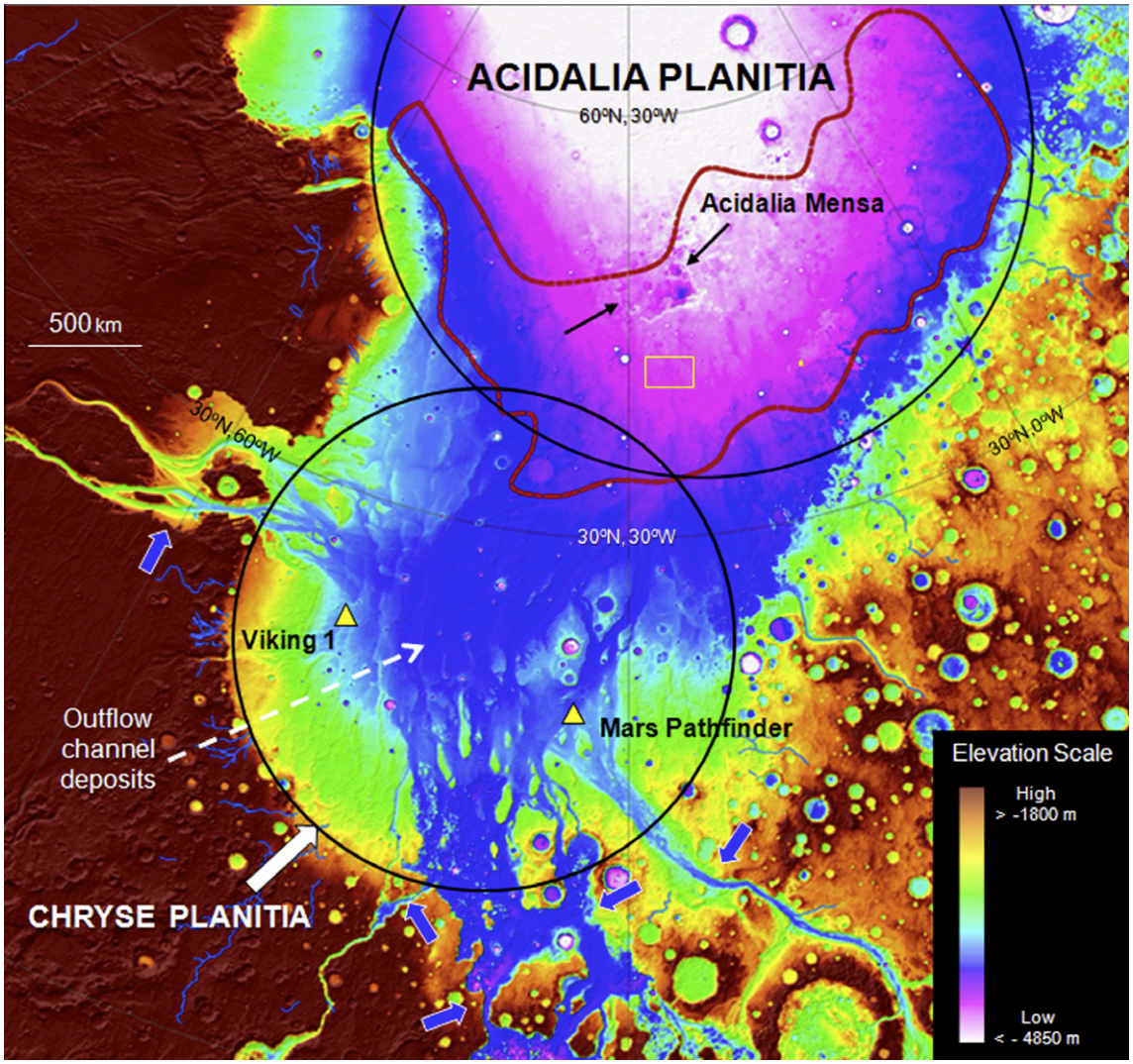

Fig. 1. Chryse–Acidalia embayment (polar projection). Approximate locations of proposed Acidalia and Chryse impact basins (Frey, 2006) are shown by black circles on a basemap of stretched MOLA topography. Previous landing sites are indicated by yellow triangles. Thick dark blue arrows point major outflow channels. Thin blue lines are channels mapped by Carr and provided by the U.S. Geological Survey in the MarsGIS DVD v. 1.4. The "Generalized Area of Occurrence" of the Acidalia mounds is outlined by red dashed line. This outline was determined by mapping the regional distribution of dark circular features in THEMIS Nighttime IR, as described in Section 3.2.1. The yellow rectangle is the area of Fig. 7E. Scale is measured at 40°N.

Science Experiment (HiRISE) on Mars Reconnaissance Orbiter (MRO) have allowed identification of associated flow-like features and internal structure in some mounds. In addition, data from the Compact Reconnaissance Imaging Spectrometer for Mars (CRISM) on MRO have provided new insights into the mineralogy of these structures. Alternative hypotheses for the origin of the mounds are further assessed in light of these new data. Results are most compatible with a model for their formation involving basinwide mud volcanism.

Mud volcanoes are terrestrial structures that extrude relatively low temperature slurries of gas, liquid, and rock to the surface from depths of meters to kilometers (Figs. 4 and 5). An excellent summary of their characteristics, mechanisms of mobilization, and worldwide occurrence is provided by Kopf (2002). These erupting slurries build circular to sub-circular deposits of mud and rock breccia that range in size from meter-scale lumps to mountains with diameters up to tens of kilometers and heights to 600 m. They can produce domes, cones, caldera-like forms, or relatively flat structures, and the range of morphologies is thought to reflect physical properties (such as viscosity) of the rising slurries as well as proportions of gas, liquid, and sediment in the extruded materials. Mud volcanoes are well known from surface mapping where they occur on land, and from seismic interpretation tied to well data, where they occur in the subsurface. Thousands of mud volcanoes have been identified globally. They have been documented in more than 40 onshore and offshore localities, and are particularly abundant in Azerbaijan and the Caspian Sea (Hovland et al., 1997; Kopf, 2002; Deville et al., 2003; Milkov and Sassen, 2003; Murton and Biggs, 2003; Stewart and Davies, 2006; Evans et al., 2008). Most have been described from onshore and shallow water localities, but recent work suggest that tens of thousands may occur on continental slopes and abyssal plains (Deville, 2009).

Mud volcanoes occur in fluid-rich basins having thick accumulations of rapidly-deposited, fine-grained sediments. Upward mud flow is related to buoyancy of the muddy and fluid-rich sediments, compared to the surrounding rocks. This type of setting is also commonly associated with the occurrence of petroleum, as conditions that favor accumulation of rapidly-deposited muds also favor concentration and preservation of organic materials that comprise source rocks for many petroleum systems (Schieber, 2003; Potter

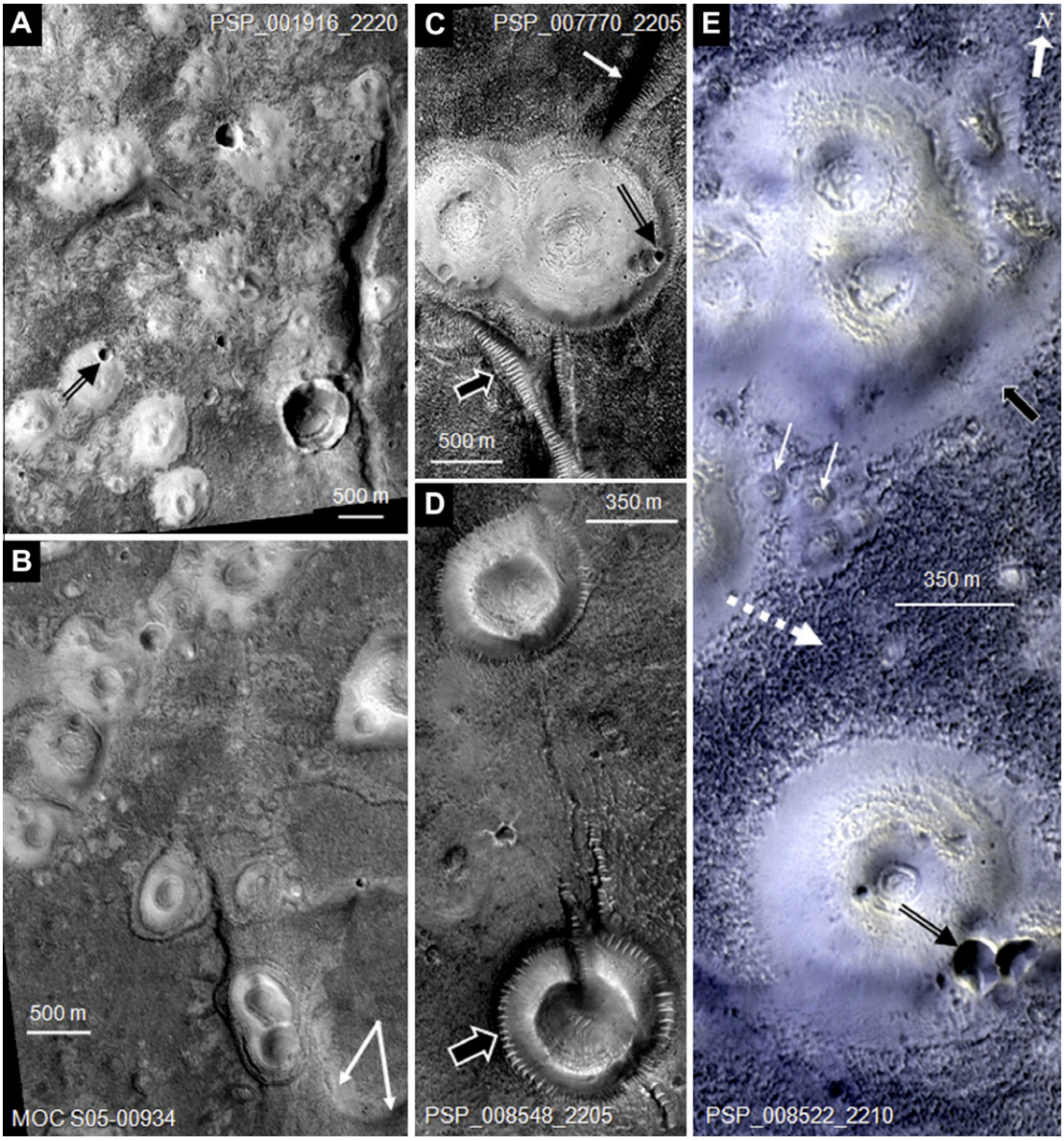

Fig. 2. High-albedo mounds in Acidalia. (A) Pitted mounds with irregular clustering. Double-tracked black arrow points to small impact crater on one of the mounds. (B) Mounds with concentric crestal depressions and moats; many are aligned along polygon boundaries or within polygon troughs. White arrows point to edge of a polygon. (C) Mounds with marked concentric structures on their crests. White arrow points to edge of a polygon. Black arrow points to dunes within the troughs between polygons. Double-tracked black arrow points to small impact crater on one of the mounds. (D) Mounds with pronounced moats and large crestal depressions. Arrow points to dunes within moat. (E) Mounds illustrating generally smooth surface textures, central depressions with muted concentric forms, well-defined peripheries (mound in lower part of image) and apron-like extensions of the smooth, high-albedo surface material onto the plains (black arrow on flank of mounds in upper part of image). Knobby texture and darker albedo of the plains material are illustrated by the dashed, bold white arrow. Double-tracked black arrow points to small impact crater on one of the mounds. North is up in all images except (E). Centerpoints of images: (A) PSP_001916_2220, 41.8°N, 332.5°E; (B) MOC S05-00934, 41.65°N, 337.78°E; (C) PSP_007770_2205, 40.0°N, 345.6°E; (D) PSP_008548_2205, 40.1°N, 341.6°E; and (E) PSP_008522_2210, 40.7°N, 332.6°E.

et al., 2005; Ware and Ichram, 2006). Upward movement of buoyant mud in the subsurface is commonly focused in zones of weakness along faults, fractures and anticlinal structures near the surface. On Mars, mud volcanoes would indicate sites that have been rich in gas, liquid, fine-grained sediments, and possibly organic materials.

2. Geologic setting

Acidalia Planitia is part of the northern lowlands of Mars (Fig. 1). It is centered at about 55°N, 338°E and extends nearly 3000 km in an east–west direction. It lies between Chryse Planitia to the south, the Tharsis volcanic province to the southwest, Arabia Terra to the southeast, and the North Polar province to the north.

Work by Frey (2006, 2008) has suggested that the lowlands were formed in part by several very large impacts that occurred early in the history of Mars, perhaps during the martian equivalent of a late heavy bombardment, about 4 billion years ago. Remnants of those partially buried impact basins are seen in quasi-circular depressions mapped by Frey. Chryse and Acidalia are both proposed to be large impact basins of this type. Others have suggested that the crustal dichotomy between the northern lowlands and southern highlands was the result of a giant impact, even earlier in the history of the planet (Andrews-Hanna et al., 2008; Marinova et al., 2008). If this occurred, then the Chryse and Acidalia basins

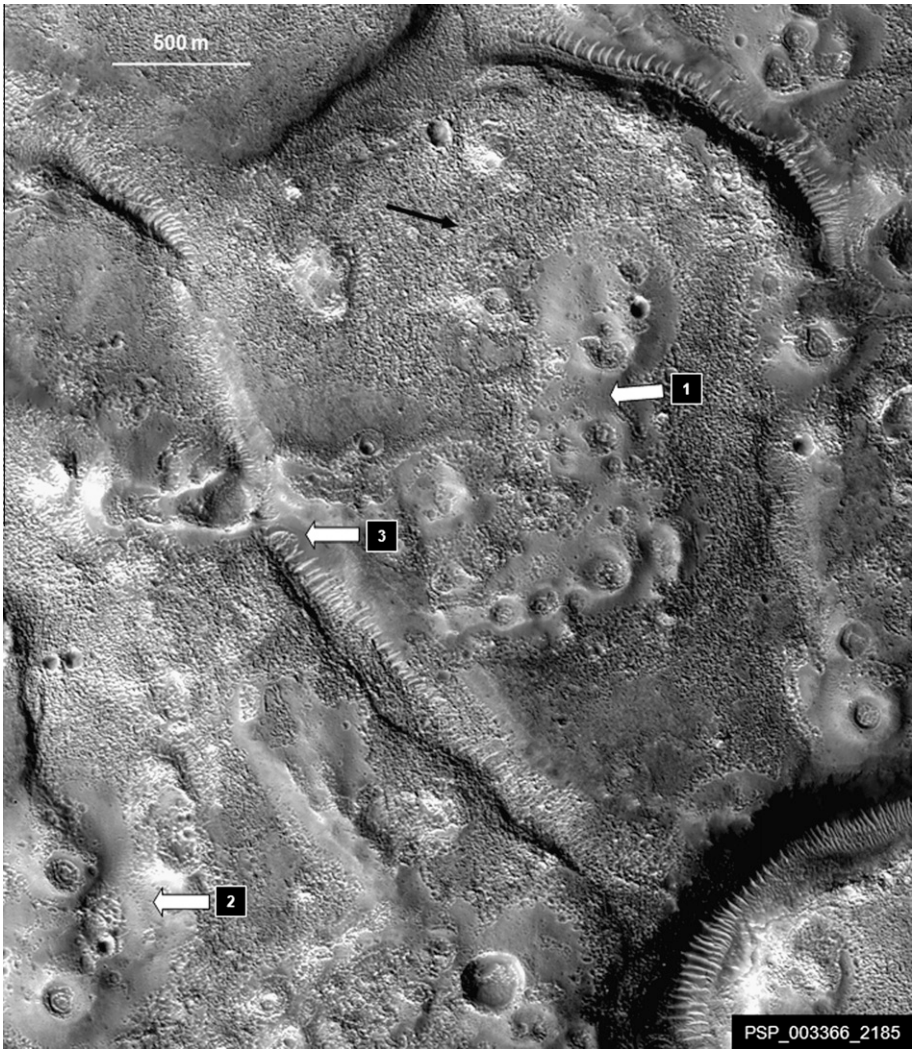

Fig. 3. Multiple mounds in region of prominent giant polygons. White arrows illustrate areas where material of the mounds appears to coalesce. The albedo of these mounds is similar to that of the plains, though the surface texture of the mounds is smoother than the knobby texture of the plains (black arrow). Well developed dunes can be seen in most of the troughs between polygons. North is up. Centerpoint of PSP_003366_2185 is 38.1°N, 347.2°E.

may have been superposed on that very early lowlands setting. Fig. 1 illustrates approximate locations of the proposed Chryse and Acidalia impact basins and shows also that the northeast rim of the Chryse basin overlaps with the southwest rim of Acidalia.

Together, Chryse Planitia and Acidalia Planitia form an embayment in the Northern Plains that was the focal point for deposition of sediments transported through the Hesperian outflow channels. Previous work has suggested that massive floods may have been delivered to the lowlands through these channels (Fig. 1) which debouch into Chryse Planitia at its southern and western perimeters (Golombek et al., 1995a,b; Rice and Edgett, 1997). Streamlined islands near the north northeastern end of Chryse suggest that water from these floods may have spilled over into Acidalia (Scott et al., 1991; Rotto and Tanaka, 1995; Rice and Edgett, 1997). Others consider that as a result of the outflow floods, Chryse, Acidalia and possibly the entire northern lowlands were under water at one time (Parker et al., 1989, 1993; Scott et al., 1991, 1995; Baker et al., 1991; Rice and Edgett, 1997).

The streamlined islands in Chryse can be seen in the remnants of channel deposits imaged in the stretched MOLA image of Fig. 1. These islands suggest that spillover into Acidalia probably occurred in the region of overlap between the two basins. Near this point, the downstream slope increases. Within Chryse, in a downstream direction approaching the northeastern rim of the basin, depths increase about 200 m over a 500 km distance; in contrast, continuing downstream into Acidalia, depths increase by 400–500 m over a 500 km distance. Assuming that regional topographic trends imaged today are similar to topography during the Hesperian floods, the Chryse basin would comprise the shallower portion of the embayment (with elevations from −3200 m to −4000 m) and Acidalia would comprise the deeper portion (with elevations from −4000 m to −5100 m).

Earlier work (Rice and Edgett, 1997) compared facies within just the Chryse Basin to proximal-, mid-, and distal-fans formed by sediments deposited by floods caused by abrupt drainage of ice-dammed lakes or subglacial eruptions. The distal-fan is the furthest downstream, has the finest-grained sediment, and is characterized by a relatively low gradient. The area of our work overlaps with the distal-fan facies described by Rice and Edgett and continues downstream through a region of higher gradients into Acidalia.

We use the terms distal and proximal in a more general sense, with regard to the combined Chryse–Acidalia embayment and relative to the points of sediment debouchment into Chryse. Thus, in our work, "proximal" is used to refer to all the channel sediments of the entire Chryse fan system and "distal" is used to refer to the sediments in Acidalia that are further downstream and that accumulated by the proposed spillover from Chryse into Acidalia.

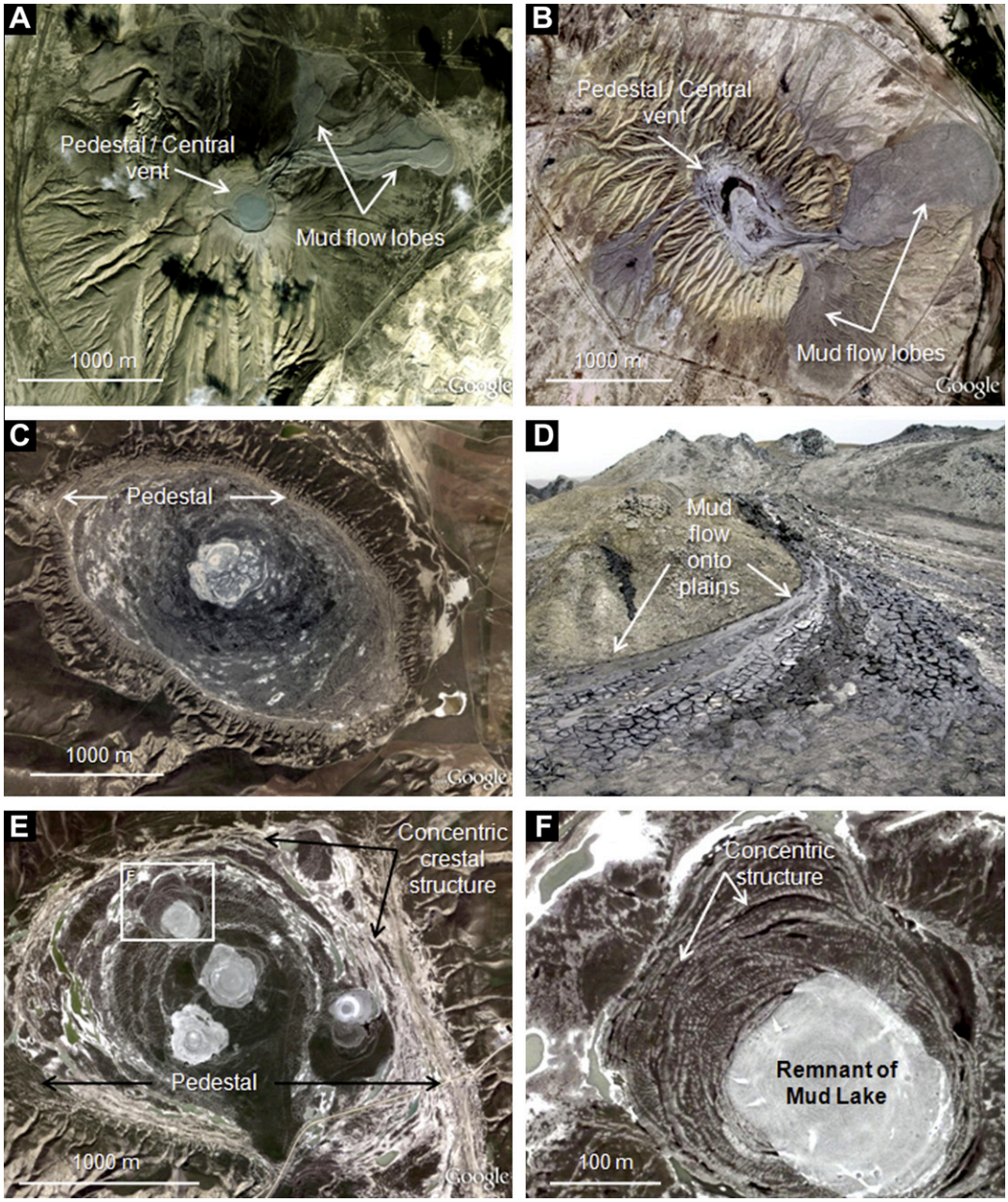

Fig. 4. Mud volcanoes in Azerbaijan. (A and B) Large, mountainous mud volcanoes. (A) Bozdag-Guzdek mud volcano. (C) Mud volcano with nearly flat, pedestal-like crest and a central high-albedo, sub-circular patch. (D) Mud flow onto the plains from the Dashgil mud volcano. (E) Mud volcano with nearly flat, pedestal-like crest, concentric crestal structure defined by high-albedo material, and several high-albedo, sub-circular patches. Rectangle shows area of detail in (F). (F) Detail of area in rectangle in (E) illustrating fine-scale, concentric surface structure and one of the high-albedo patches. North is up in all images. Centerpoints of images: (A) 40.380°N, 49.611°E; (B) 39.921°N, 49.265°E; (C) 40.372°N, 48.987°E; (D) 39.996°N, 49.402°E; and (E) 40.380°N, 49.611°E.

The geologic map of the Northern Plains (Tanaka et al., 2005) shows most of Acidalia to be covered by the Early Amazonian Vastitas Borealis Interior and Marginal units (Fig. 6). These units are considered to be "a mixture of undifferentiated Noachian to Hesperian materials and local outflow-channel sediments that have been altered by *in situ* permafrost-related processes such as cryoturbation, desiccation, and thermokarst involving near-surface deformation and mass movements aided by subsurface volatiles . . ." (Tanaka et al., 2003). The Vastitas Borealis units also are viewed as potential paleo-ocean deposits resulting from reworking of outflow sedimentation by mass flow, sedimentary volcanism and periglacial modification perhaps due to repeated warming events (Tanaka et al., 2005). Kreslavsky and Head (2002) note that Vastitas Borealis deposit may comprise a sublimation residue from frozen, ponded water bodies and that it may lie on Hesperian volcanic ridged plains. Within the Vastitas Borealis Interior Unit are numerous rimless "ghost" craters – features that appear to be remnants of impact craters buried by the Unit and which may attest to a substantial thickness for this Unit. A small region near the southwestern limit of the "Generalized Area of Occurrence" of the mounds (Fig. 1) corresponds to the Chryse Planitia 2 Unit, of proposed Early to Late Hesperian age (Tanaka et al., 2005).

Near central Acidalia Planitia, a topographically high platform, Acidalia Mensa (Fig. 1), stands a few hundred meters above the plains (Tanaka and Banerdt, 2000). This platform extends about 150–285 km in a north–south direction and 200–350 km in an east–west direction. The geologic map of the Northern Plains

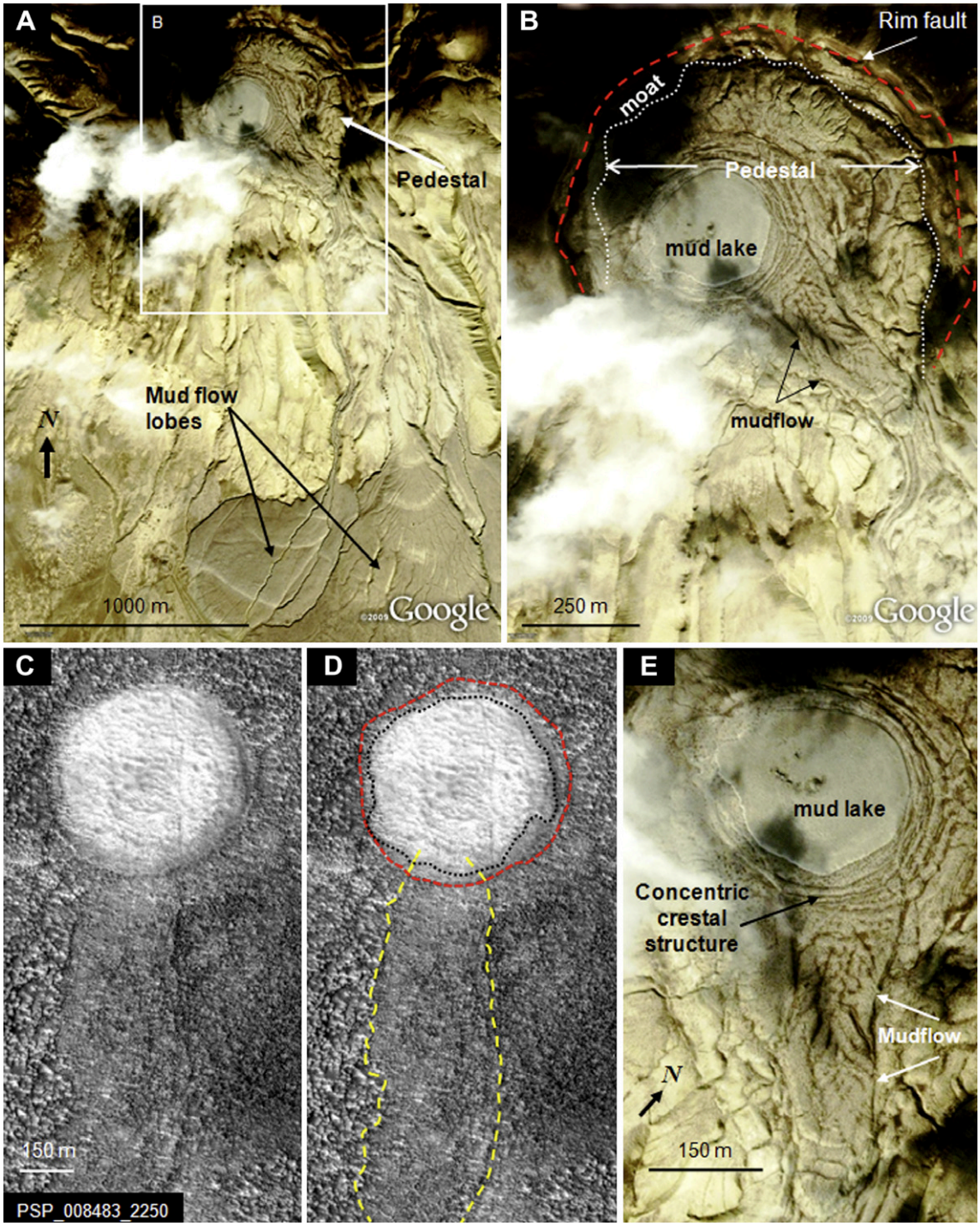

Fig. 5. Qaraqus-Dagi "moat-and-pedestal" mud volcano in Azerbaijan and comparison with a mound in Acidalia. (A, B, and E) Qaraqus-Dagi mud volcano. Interpretation adapted from Evans et al. (2008). Rectangle in (A) shows area of (B). (C and D) Acidalia mound and associated structures. (C) Uninterpreted. (D) Interpreted; yellow dashed lines outline potential remnant mud flow with defined lateral boundaries and slightly smoother texture than the plains to the west. Red dashed line follows possible rim fault. Black dotted line outlines possible pedestal edge or perimeter of an equivalent of a mud lake. (E) Close-up of central part of pedestal of Qaraqus-Dagi mud volcano showing the mud lake, the concentric crestal structure (relics of previous mud lakes), and a remnant mudflow. Note that the orientation of north has been altered to facilitate comparison with the Acidalia structure in (C and D). Centerpoint of pedestal of Qaraqus-Dagi mud volcano, 40.240073°N, 49.507123°E. Centerpoint of PSP_008483_2250 is 44.4°N, 317.0°E.

(Tanaka et al., 2005) shows Acidalia Mensa to be comprised of the Early Noachian Nepenthes Mensae Unit, the Middle to Late Noachian Noachis Terra Unit, and the Early Amazonian Vastitas Borealis Marginal Unit. The platform has been interpreted as a product of uplift, possibly due to upwelling of volatiles (Tanaka et al., 2003).

3. Data and methodology

3.1. Data

We used many of the mosaics and data provided by the U.S. Geological Survey in their MarsGIS DVD v. 1.4, including Mars

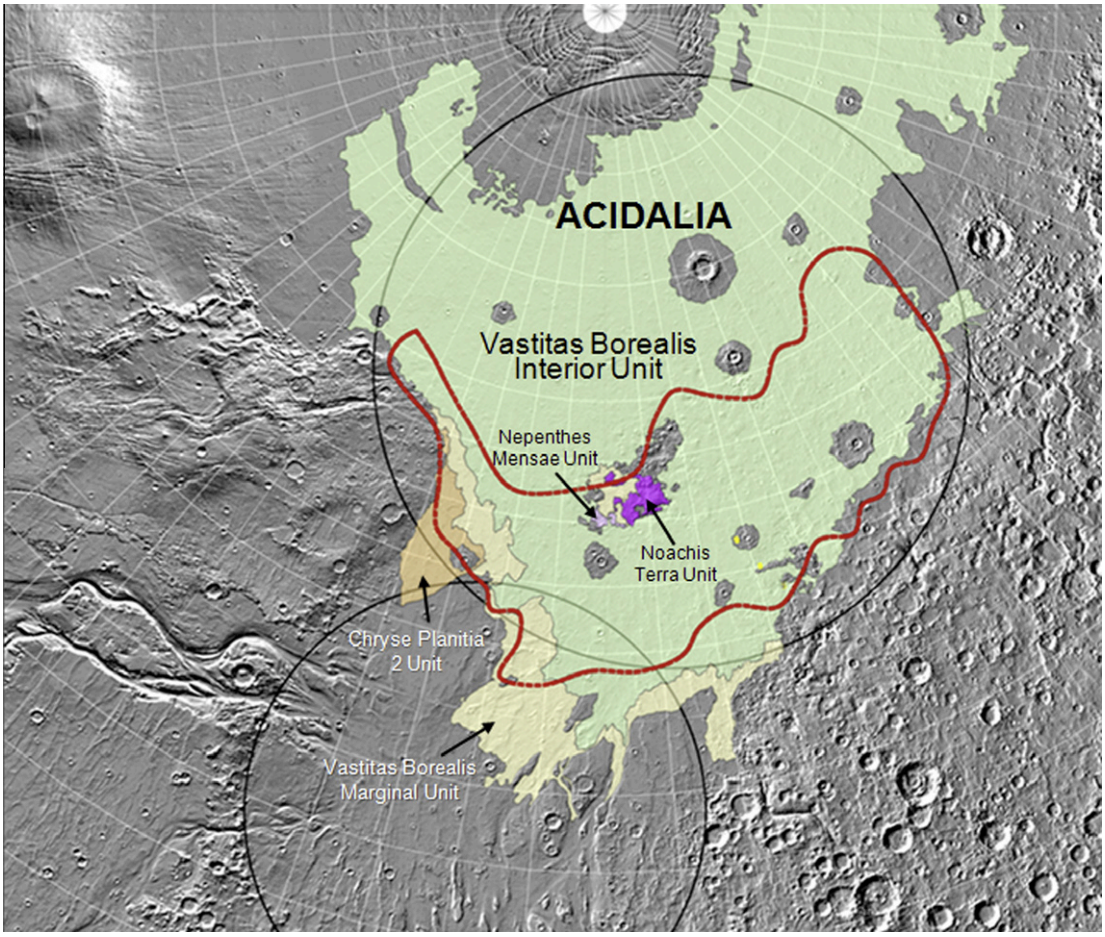

Fig. 6. Overlay of geologic units with "Generalized Area of Occurrence" of Acidalia mounds (Polar projection). Image shows the correspondence of the Vastitas Borealis Interior (pale green) and Marginal (light tan) units with the "Generalized Area of Occurrence" of the mounds (red outline) on a basemap of MOLA hillshade with 128 pixels/degree. The Noachis Terra and Nepenthes Mensae units outcrop on the Acidalia Mensa platform, and areas on this platform of multiple, coalescing mounds and apparent flows into polygon troughs tend to correlate with the Noachis Terra Unit. Geologic units are from the geologic map of the Northern Plains (Tanaka et al., 2005) and the outlines of that map as well as the MOLA basemap were provided in the MarsGIS DVD v. 1.4 created by the U.S. Geological Survey. Light gray lines are 5° latitude/longitude grid lines. For reference, the center of Acidalia is at about 56°N, 338°E.

Orbiter Laser Altimeter (MOLA) data from Mars Global Surveyor orbiter (MGS), Nighttime Infrared (IR) data from the Thermal Emission Imaging Spectrometer (THEMIS) on Mars Odyssey, and the map of Mars gravity anomalies (evaluated for the MGM1025 model from radio science investigations on MGS). We also incorporated new data from the CTX and HiRISE cameras and the CRISM spectrometer, coupled with observations of individual images from the Mars Orbiter Camera (MOC) on MGS and THEMIS Nighttime IR. We used individual THEMIS Visible (VIS) images for counting impact craters on the mounds. For reference geology, we used digital outlines of geologic units in the recent geologic map of the Northern Plains (Tanaka et al., 2005), also provided on the MarsGIS DVD v. 1.4.

3.2. Methodology

We applied a regional geologic approach coupled with detailed geomorphology to assess the significance of the mounds in Acidalia. The THEMIS Nighttime IR mosaic was selected for mapping the mounds in Acidalia, as the mounds are prominent, dark circular structures in this dataset (Fig. 7) and therefore are readily identifiable. Image data were geographically rectified and compared using ESRI's ArcGIS software. Mapping was done at a scale of 1:250,000–1:500,000.

3.2.1. Distribution of the mounds – "Generalized Area of Occurrence"

The distribution of the mounds was determined as follows: In the THEMIS Nighttime IR mosaic, individual polygons were drawn around areas with multiple dark circular structures in regions having good-quality data. In areas of poor-quality Nighttime IR data, if the presence of the mounds could be established with MOC, CTX, THEMIS Daytime IR, or THEMIS VIS image data, polygons were drawn around those areas as well. If the presence of mounds could not be established by any of the datasets, then the region was excluded. A "Generalized Area of Occurrence" was outlined by drawing a curve around all the individual polygons. This area is shown in Fig. 1 and is about 2.5×10^6 km^2. North of 50–60°, good-quality image data of all types were sparse, and regional mapping of the structures was not possible.

3.2.2. Estimates of abundance and spatial density of the mounds

Locations of more than 18,000 individual mounds were mapped (Amador et al., 2010) using the THEMIS Nighttime IR mosaic. Only circular to sub-circular features greater than 300 m diameter (3 pixels) were included, as that is the smallest structure that can be confidently identified with the 100 m/pixel resolution of THEMIS IR data. Some dark features were diffuse or more linear than circular. These were not included. Wherever possible, checks were made with MOC, HiRISE, CTX, THEMIS Daytime IR, or THEMIS VIS

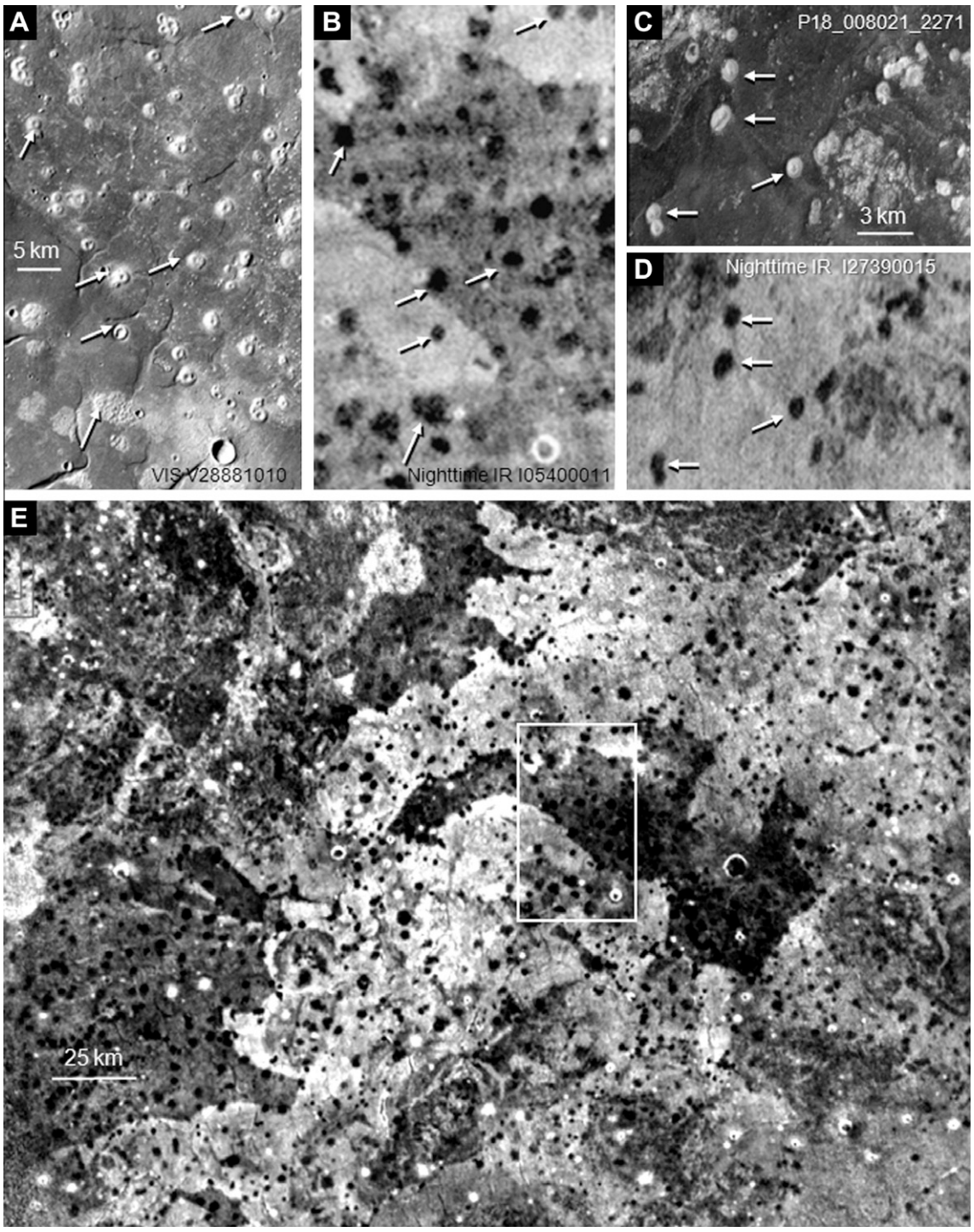

Fig. 7. Abundance and density of mounds in Acidalia Planitia. (A and B) Comparison of high-albedo mounds as seen in THEMIS VIS (A) with THEMIS Nighttime IR response (B) of the same area. Arrows point to the same mounds in each image. (C and D) Comparison of high-albedo mounds as seen in CTX image (C) with THEMIS Nighttime IR response (D) of the same area. Arrows point to the same mounds in each image. Comparisons in (A–D) illustrate the one-to-one correspondence of the high-albedo mounds with the dark circular patches in Nighttime IR. (E) THEMIS Nighttime IR of an area illustrating density and abundance of mounds. White rectangle is the location of (A) and (B). The location and relative size within Acidalia of (E) is shown by the yellow rectangle in Fig. 1. Source for (E) is the THEMIS Nighttime IR mosaic provided by the U.S. Geological Survey in the MarsGIS DVD v. 1.4. North is up in all images. Centerpoints of images: (A) VIS V28881010, 41.008°N, 334.115°E; (B) I05400011, 47.209°N, 330.74°E; (C) P18_008021_2271, 47.13°N, 331.15°E; (D) I27390015, 44.4°N, 331.4°E; and (E) 41.03°N, 333.88°E.

image data to ascertain that the dark circular features being mapped corresponded to the mounds.

This mapping exercise did not cover the entire "Generalized Area of Occurrence" of the mounds (total area in which the presence of the mounds has been established). Rather, about 45% of the area (estimated visually) was covered in this phase of the work. Extrapolating to the entire "Generalized Area of Occurrence" would result in an estimate of about 40,000 mounds having diameters of 300 m or greater. This assumes that a similar density of features occurs in the unmapped areas, an assumption that seems reasonable based on spot-checking in several of the unmapped regions using THEMIS Nighttime or Daytime IR, THEMIS VIS, MOC, or CTX images.

Spatial densities (Table 1) of the mounds were estimated by counting individually mapped mounds in three different, similar-sized (~22,000–29,000 km^2) areas (Amador et al., 2010). These three areas include (1) a region in eastern Acidalia where the mounds occur along ridges in concentric, arcuate features (Centerpoint 44°N, 318°E); (2) a more central area, where the mounds are particularly abundant and occur in association with muted giant polygons that cross parts of Acidalia (Centerpoint 41°N, 334°E); and (3) a region in the south–southeast of Acidalia where the mounds occur in association with prominent giant polygons (Centerpoint 41°N, 348°E). For each of these areas, the mapped mounds were counted and the number of mounds per 1000 km^2 in each region was calculated.

3.2.3. Estimates of mound diameter and height

Diameters of 150 mounds were measured using the THEMIS Nighttime IR image mosaic (Amador et al., 2010); these 150 included representatives from each of the three regions used for density. Height was estimated from three-dimensional photogrammetry of a HiRISE stereo pair (PSP_002233_2225 and PSP_002866_2225; Centerpoint for each, 42.1°N, 319.3°E). Photogrammetry was performed by staff of the Johnson Space Center Image Science and Analysis Group, using workstations equipped with StereoGraphics CrystalEyes™ Viewers for high resolution, stereoscopic 3D visualization and measurement.

4. Description of the Acidalia mounds

4.1. Characteristics

The mounds (Figs. 2 and 3) are circular to sub-circular structures, hundreds of meters to several kilometers in diameter. Most are characterized by high albedo relative to the surrounding plains (Fig. 2), though there is a range of albedos such that some mounds are very bright compared to the plains and others are similar in albedo to the plains (Fig. 3). Many mounds appear as domes, though the shapes can vary from steeper-sided cones to concave caldera-like structures to nearly flat, pancake-like structures. The mounds typically have a smooth surface texture that contrasts with the more rugose texture of the knobby plains-forming material (Figs. 2 and 3). The surfaces of the mounds may be pitted or unpitted (Figs. 2 and 3), and the crests of many mounds exhibit muted, concentric ring-like features (Figs. 2 and 8). Some mounds are encircled by moats (Fig. 2) and some have apron-like extensions where the smooth surface material of the mounds appears to extend over the knobby material of the plains, resulting in a mesh-like appearance (Fig. 8). The peripheries of many are well defined by the limit of the smooth, high-albedo material.

In THEMIS Nighttime IR, the mounds are considerably darker than the plains (Fig. 7), forming very dark, well-defined circular features; this includes mounds with both high albedo and those with relatively low albedo. In Nighttime IR, the plains of southern Acidalia are comprised of both light and dark material and the mounds overlie both types of materials. Thermal inertia of the mounds was estimated by Farrand et al. (2005) to be in the range

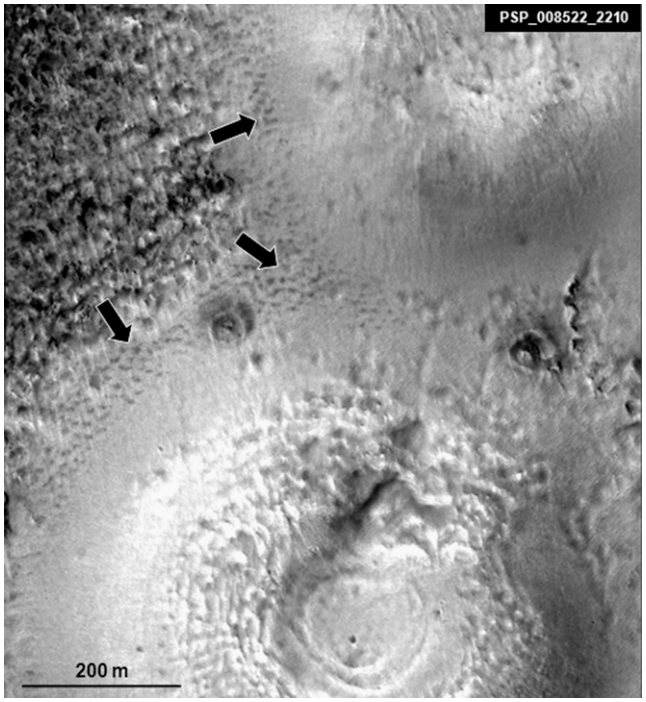

Fig. 8. Apron-like extension of high-albedo material from an Acidalia mound onto the plains. Arrows point to mesh-like texture where the high-albedo surface material of the mound interacts with the knobby texture of the plains. North is up. Centerpoint of PSP_008522_2210 is 40.7°N, 332.6°E.

190–240 thermal inertia units (tiu; defined as J m^{-2} s$^{-1/2}$ K^{-1}), using a TES-derived thermal inertia map (Mellon et al., 2002) and the THEMIS Nighttime IR images. Based on their work, Farrand et al. (2005) noted that the mounds have an overlapping but slightly lower range of thermal inertia than the surrounding plains.

Table 1 shows the diameters of the 150 mounds that were measured in three separate areas of southern Acidalia. The diameters range from about 300 m to 2200 m, with an average of 830 m. For comparison, Frey and Jarosewich (1982) measured diameters of 1520 cones in southern and eastern Acidalia and obtained a range of ~400–1500 m. Farrand et al. (2005) calculated sizes for several of these features: for the domes, they reported a mean basal diameter of 774 m; for the cones, they reported a mean basal diameter of 455 m and heights of 35–65 m (from MOLA altimetry). Our work using 3D photogrammetry of two mounds with diameters ~650 m and 750 m (in HiRISE stereo pair PSP_002233_2225 and PSP_002866_2225) yielded a maximum rim height of approximately 180 m.

4.2. Occurrence, abundance, and spatial density

The mounds in Acidalia are located within the "Generalized Area of Occurrence," which is ~2.5 × 10^6 km^2 and nearly coincident with the southern half of the proposed (Frey, 2006) Acidalia

Table 1
Spatial density and average diameters of mounds in different regions of Acidalia.

Location	Terrain	Centerpoint	Area (km^2)	# of mounds	Spatial density (mounds/1000 km^2)	Average diameter of mounds (# mounds measured)[a] (m)
1	Arcuate Ridges	44°N, 318°E	28,823	1499	52	1020 (31)
2	Muted Polygons	41°N, 334°E	22,239	2546	114	718 (97)
3	Prominent Polygons	41°N, 348°E	22,790	476	21	1060 (22)

[a] Diameters were measured on subsets of mounds in 1000 km^2 areas within each of the different locations; numbers in parentheses are the number of mound diameters measured.

impact basin (Fig. 1). Fig. 7 illustrates the abundance and density of the mounds, as imaged in the THEMIS Nighttime IR mosaic provided by the USGS in their MarsGIS DVD. As described in the Methodology Section, estimates from regional mapping suggest that 40,000 mounds with diameters greater than 300 m may exist in the "Generalized Area of Occurrence." Since many of the mounds seen in MOC, THEMIS VIS, CTX, or HiRISE images have diameters less than 300 m, the actual number of mounds within the "Generalized Area of Occurrence" is likely to be considerably greater than 40,000.

The mounds occur singly, in pairs, in irregular clusters and in chains (Figs. 2 and 3). The chains may be relatively straight, overlying troughs between the giant polygons that cross much of southern and southeastern Acidalia or they may be curvilinear, aligned along ridges in arcuate features within a region in southwestern Acidalia referred to as the "thumbprint terrain" (Tanaka et al., 2005). In some areas with many closely-spaced mounds, the smooth material of the mounds appears to coalesce (Fig. 3).

Spatial densities of the mounds in three regions within Acidalia (Table 1) range from a low of 21 mounds/1000 km^2 in the south–southeastern region that is traversed by prominent giant polygons to a high of 114 mounds/1000 km^2 in the more central area with muted giant polygons (Amador et al., 2010). Frey and Jarosewich (1982) report spatial densities in eastern Acidalia/Cydonia of about 5–78 structures/1000 km^2. Skinner and Mazzini (2009) report a much higher spatial density of 358 mounds/1000 km^2 in Acidalia for mounds with diameters of 400–600 m. However, comparison of the density figure of Skinner and Mazzini with our density estimates is difficult since the areas used by Skinner and Mazzini are not reported, and spatial densities in Acidalia are variable enough (e.g., Fig. 7) that higher numbers could be obtained if different or smaller areas were used.

The densities that we measured correlate somewhat with average diameters in that the area with the lowest density (21 mounds/1000 km^2) contains mounds with largest average diameter of 1060 m; similarly, the area with the highest density (114 mounds/1000 km^2) has mounds with the smallest average diameter of 718 m (Table 1). A similar inverse relationship between spatial density and mound diameter was found by Frey and Jarosewich (1982).

4.3. Indications of flow

There are several examples of features associated with the Acidalia mounds that might be products of flow from the mounds (Figs. 9 and 10). In Fig. 9, several flow-like forms are seen to emanate from individual mounds. In Fig. 10, flows from four mounds appear to have spilled into a polygon trough. Fig. 10B, in particular, shows what appears to be material from the mound surface traversing both the side and the floor of the trough.

Fig. 11 illustrates features possible flow features associated with mounds on the Acidalia Mensa platform. In this figure, troughs intersect the mounds. These troughs have some features in common with the well-studied giant polygons of the plains, but the tectonic history of the troughs on Acidalia Mensa may be unique to that platform. The internal structure of the mound at the lower left of Fig. 11A is exposed in cross-sectional view by the trough cut and appears to consist of stacked cones (Fig. 11B). A similar internal architecture has been described from 3D seismic studies of kilometer-scale mud volcanoes in the South Caspian Sea, where the stacked conical architecture is thought to have formed from repeated episodes of fluid-mud expulsion (Stewart and Davies, 2006; Evans et al., 2007). A mound in the lower right of Fig. 11A, also located in a trough, has similar internal structure

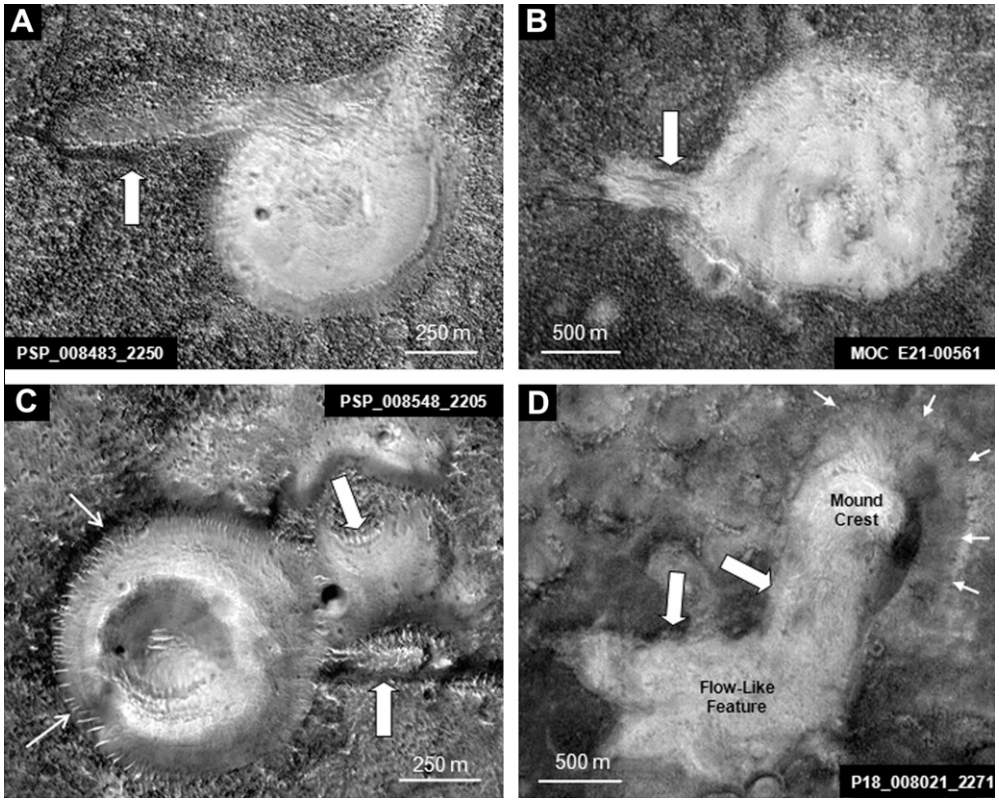

Fig. 9. Lobate and flow-like features associated with Acidalia mounds. (A) Lobate feature (arrow) extending from mound. (B) Flow-like extension (arrow) of high-albedo material of mound. (C) Flow-like features (thick arrows) emanating from a mound with a well-developed moat (thin arrows). (D) Mound on the Acidalia Mensa platform with apparent flow (thick arrows) onto the plains. Thin arrows outline periphery of mound. North is up in all images. Centerpoints of images: (A) PSP_008483_2250, 44.4°N, 317.0°E; (B) MOC E21–00561, 42.72°N, 320.94°E; (C) PSP_008548_2205, 40.1°N, 341.6°E; and (D) P18_008021_2271, 47.13°N; 331.15°E.

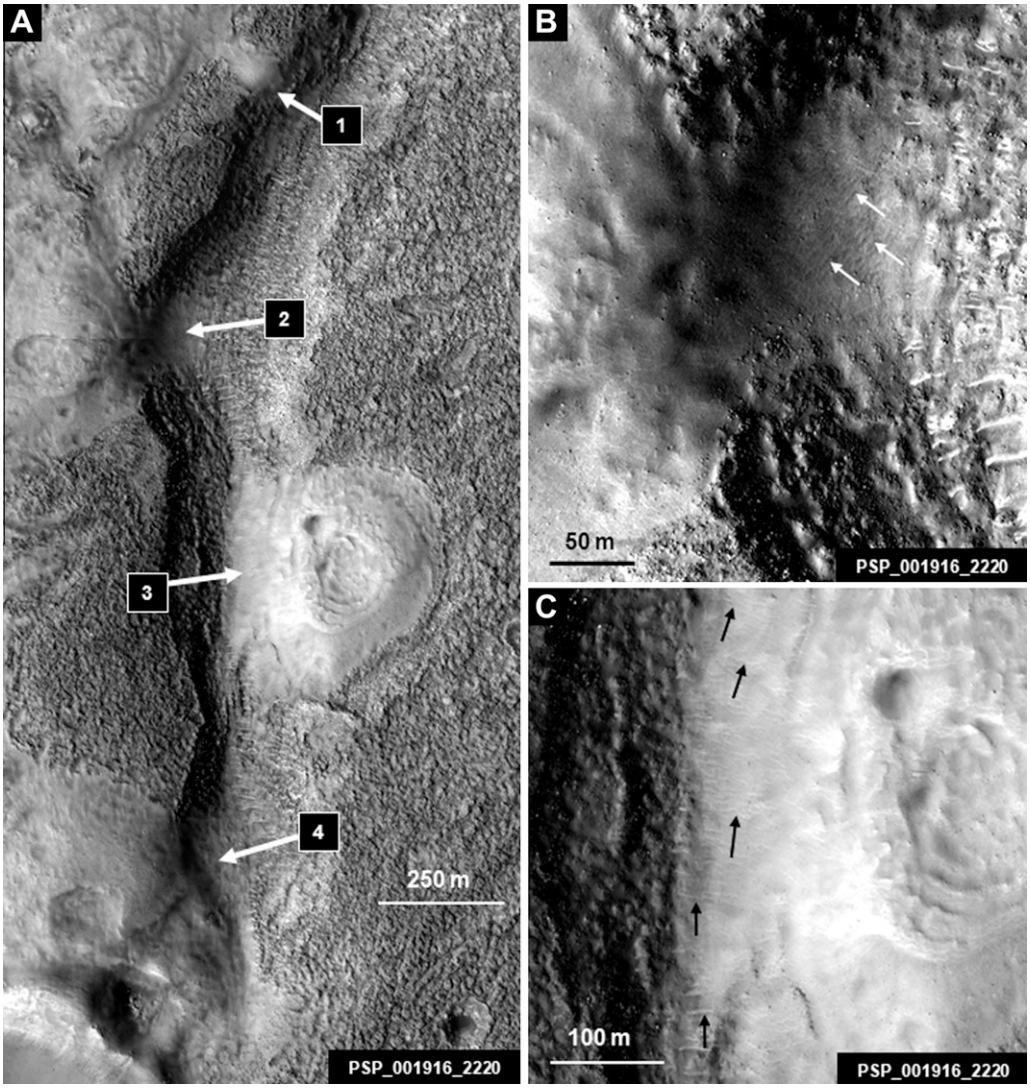

Fig. 10. Four mounds at edge of polygon trough with apparent flow into the trough. (A) Arrows point to apparent flow from each of the four mounds. (B) Detail of feature Number 2 in (A) showing flow-like materials extending from the edge of the mound onto the sides and floor of the trough; arrows point to possible flow textures within high-albedo material. (C) Detail of feature Number 3 in (A); arrows point to possible flow textures within high-albedo material. North is up in all images. Centerpoint of PSP_001916_2220 is 41.8°N, 332.5°E.

exposed in plan view. The troughs between the mounds contain material that is contiguous with, and similar in albedo, texture, and Nighttime IR response to the material inside the mounds (illustrated by the inset in Fig. 11A as well as in Fig. 11B and C).

These observations might suggest that the material comprising the mounds and that filling the troughs had a similar origin. If the mounds on Acidalia Mensa are mud volcanoes, then it may be that mud has both filled the troughs and built the mounds. This interpretation is consistent with the regional geologic setting. However, the trough-filling material also resembles snow-rich mantling in the mid-latitudes (e.g., Christensen, 2003), ballistically-emplaced materials, and valley fill in the Highlands, and since only one image illustrates these features, other interpretations remain possible.

4.4. Age of mounds in the plains of Acidalia

Geological relationships suggest that most of the Acidalia mounds are of Amazonian age. The Amazonian is estimated to range from ~3 Ga to the present, based on martian crater densities (Hartmann and Neukum, 2001; Neukum, 2008), and the Early Amazonian is estimated to extend from ~3 to 1.75 Ga, though there are alternative interpretations of the cratering record (McEwen et al., 2005). The majority of the mounds are located on plains material (Figs. 2, 3, and 12) mapped as the Vastitas Borealis Interior Unit or Vastitas Borealis Marginal Unit (Fig. 6), both of which are placed within the Early Amazonian (Tanaka et al., 2005).

Acidalia mounds exhibit sharp-rimmed depressions that are morphologically distinct from the ubiquitous summit pits. Examples are shown in Fig. 2A, C, and E. These sharp-rimmed depressions were interpreted as impact craters and were used to roughly estimate the ages of the mounds.

Mounds and craters were counted on three THEMIS VIS Daytime images which show large numbers of mounds on plains and polygons (V11622007, Centerpoint 39.32°N, 331.33°E; V13219004, Centerpoint 38.65°N, 342.52°E; and V28881010, Centerpoint 41.01°N, 334.11°E; spatial resolution 38 m, 38 m, and 19 m, respectively). Only craters larger than 250 m in diameter and mounds larger than 300 m in diameter were counted, due to concerns that smaller craters, particularly degraded ones, might not be recognizable. While higher-resolution images such as those from HiRISE resolve smaller craters, current HiRISE coverage across Acidalia is too limited to provide statistically meaningful counts.

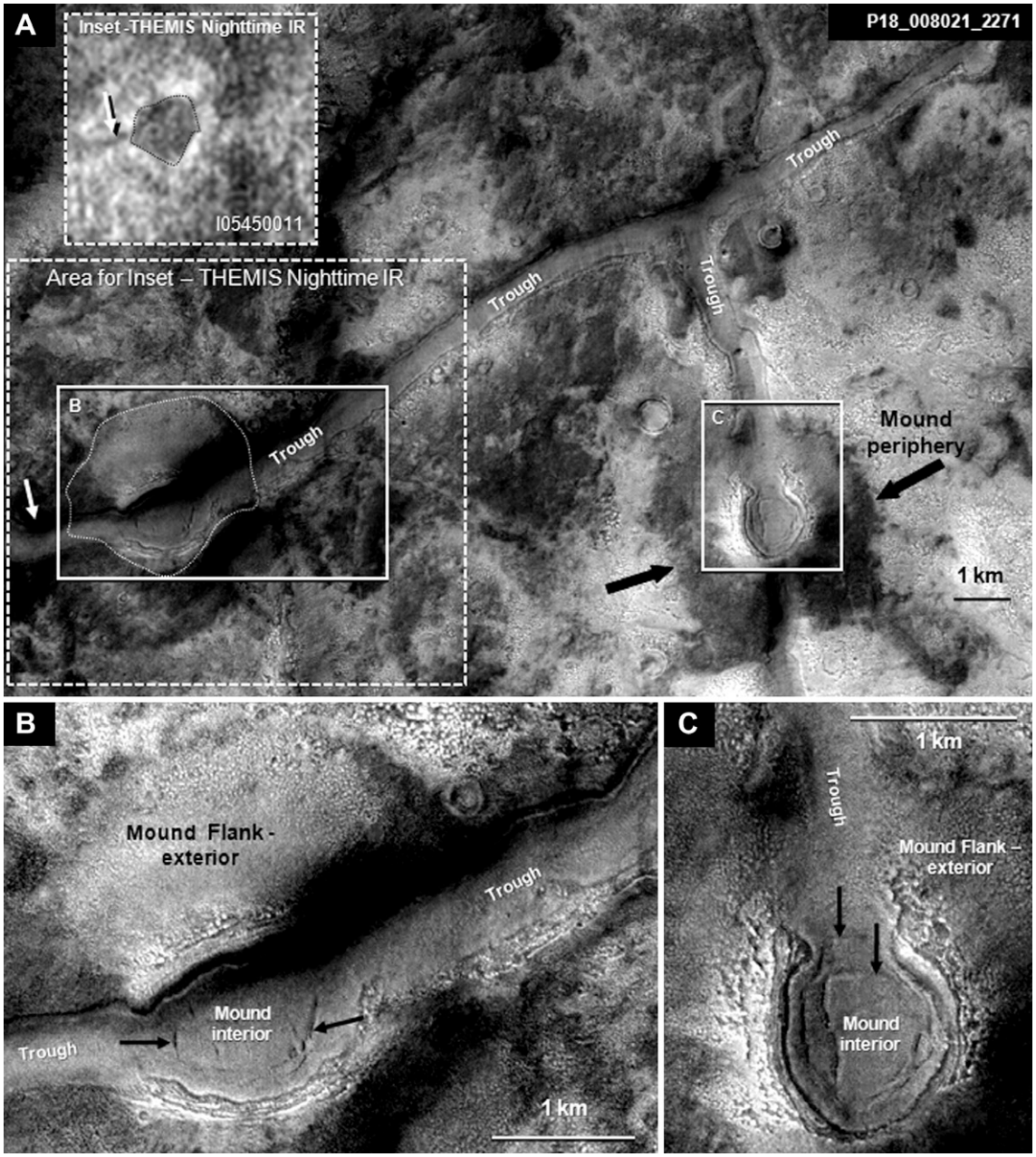

Fig. 11. Mounds and troughs on the Acidalia Mensa platform. (A) Overview in CTX image. Solid white rectangles enclose mounds cut by troughs and show areas of detail in (B) and (C). Lower dashed rectangle in (A) shows area for which THEMIS Nighttime IR data is shown (upper dashed rectangle, titled "inset – THEMIS Nighttime IR"). White arrows in both dashed rectangles point to the same spot. The thin white dotted line in Rectangle B and the thin black dotted line in the inset show the periphery of the mound. Thick black arrows illustrate periphery of mound of Rectangle C. (B) Detail of Rectangle B in (A). Arrows point to internal conical structure of mound where it is exposed in cross section by the trough cut. (C) Detail of Rectangle C in (A). Arrows point to internal structure of mound where it is exposed in plan view by the trough. Regional setting of Acidalia Mensa is shown in Fig. 1. North is up in all panels. Centerpoint of P18_008021_2271 is 47.13°N, 331.15°E.

Altogether 155 craters (250 m–2.31 km diameter) were tabulated in an area totaling 3933 km^2. Of these, 31 craters are larger than 500 m in diameter. The size/frequency distributions for craters larger than 500 m are consistent with the estimated early Amazonian age for the Northern Plains (Tanaka et al., 2005), based on the isochrons of Hartmann (2005). Our total counts for craters 250–500 m in diameter are deficient, possibly due to erosion that preferentially destroys smaller craters. An early Amazonian age for the areas counted indicates that they are representative of the larger study area.

We identified a total of 333 mounds larger than 300 m in diameter on the three THEMIS VIS images, yielding a spatial density of 85 mounds/1000 km^2. This value is close to the spatial density reported in our larger survey of mounds in areas of muted polygons (Table 1). The mean diameter of these mounds is 630 m (±150 m standard deviation), again close to the value in Table 1 for mounds in regions of muted polygons. The combined area of the mounds is approximately 111 km^2.

A total of 12 probable impact craters ranging in size from 250 m to 570 m postdate these mounds. In some cases the craters are completely contained within the perimeters of the mounds, and in some cases the craters overlap the mound edges. In order to account for overlapping craters in our size/frequency distributions we calculated an "effective" area for each mound that extended one mound radius past the edge – giving an effective area of πd^2 or four times the actual mound area. The total effective area of

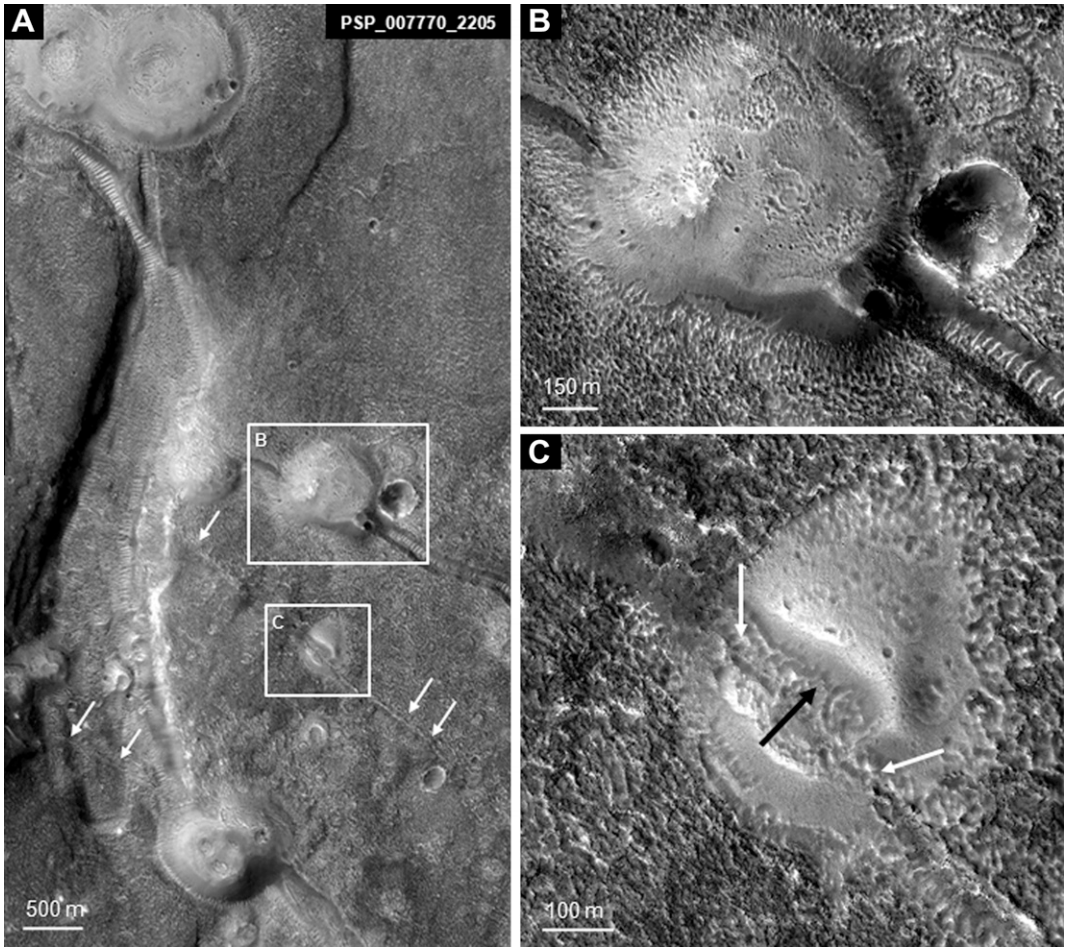

Fig. 12. Acidalia mounds associated with polygon troughs and fractures. (A) Overview. Mounds associated with a large sinusoidal polygon trough and linear features resembling fractures (arrows). Rectangles are areas of (B) and (C). (B) Detail of rectangle B in (A), showing mound overlying a polygon trough. (C) Detail of rectangle C in (A), showing mound cut by narrow, linear feature resembling a fracture. White arrows point to fracture-like feature. Black arrow points to interior of mound exposed by the fracture. North is up in all images. Centerpoint of PSP_007770_2205 is 40.0°N, 345.6°E.

the mounds is thus approximately 444 km^2. The isochron plot derived from these craters is slightly below, but statistically indistinguishable from, the plot for craters on the underlying plains.

Such a calculation is inherently imprecise, given the low number of craters and the correspondingly large statistical uncertainties. The calculation inherently assumes that the mounds in these three areas of Acidalia formed at approximately the same time. This age may be underestimated, due to incomplete preservation of craters on the mounds. Conversely, the age could be overestimated due to the presence of secondary craters within some of the counted areas.

As discussed above, the mounds clearly overlie the plains material. In addition, mounds generally postdate the giant polygons common in many areas of these plains. However, the mounds have been impacted a significant number of times. Our crater counts, given their large uncertainties, are consistent with a history of mound-formation soon after deposition of the Acidalia plains. The early history of Acidalia apparently included massive sedimentary deposition, followed shortly by large-scale polygonal fracturing and widespread sedimentary diapirism resulting in thousands of mud volcanoes.

4.5. Age of mounds on the Acidalia Mensa platform

On the Acidalia Mensa platform, some mounds lie on the Middle to Late Noachian Noachis Terra Unit. A few of these mounds are cut by troughs (Fig. 11) and must be older than the tectonic activity that formed these troughs. But, as discussed above, the troughs appear to be filled with material that appears identical to that comprising the mounds and may have flowed into the troughs from the mounds. If this were the case, it would suggest that extrusion of material from the mounds on this platform may have extended beyond the time of trough-formation. It is not clear whether these mounds are older than the mounds elsewhere in Acidalia or whether trough-formation on the Acidalia Mensa platform occurred later in time than polygon-formation throughout the plains of Acidalia.

4.6. Mineralogy

CRISM data from nine scenes that covered mounds in Acidalia were used to compare mineralogy of the domes and plains (Fig. 13). These scenes span southern Acidalia from east to west and include the Acidalia Mensa platform. Spectral responses suggest that the mounds and plains are generally similar in composition. In near-infrared (NIR) wavelengths, both show the muted mafic responses that are common in Acidalia (Salvatore et al., 2009, 2010). However, there are also indications of subtle differences. CRISM spectra of individual domes were ratioed to spectra representative of the adjacent plains in each scene (Fig. 13A). In the visible (VIS) portion of all of the ratioed spectra, the positive slopes between 0.4 and 0.65 μm suggest that the mounds have

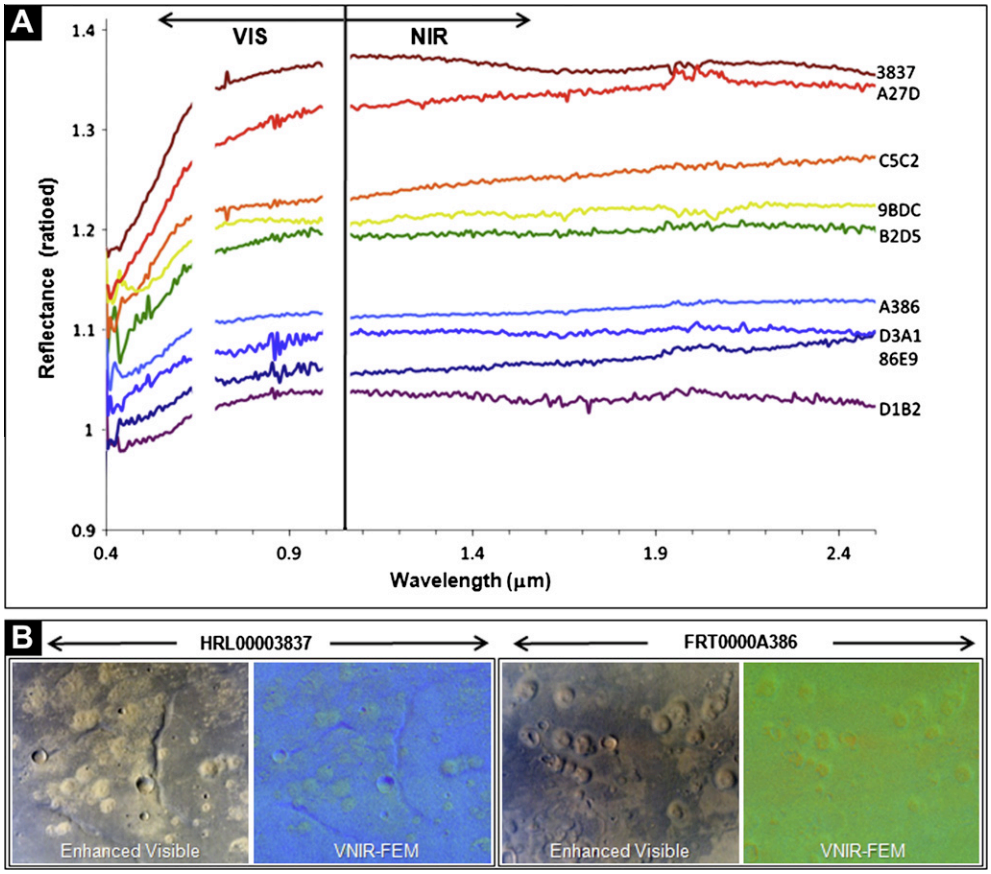

Fig. 13. CRISM data. (A) Ratio spectra of domes to representative of plains material in each image. Numbers on the right are the last four digits of the CRISM image numbers. (B) Enhanced Visible Color images and visible–near-infrared browse images for oxidized iron minerals (VNIR-FEM) for two examples of CRISM scenes in Acidalia that cover areas with mounds (http://crismmap.jhuapl.edu/details.php?data=hrl_webmap_polygons&shape=61&x=-27.47947&y=41.82618). Centerpoints of CRISM images: Image No. HRL00003837, 41.83°N, 332.52°E; Image No. HRL0000A27D, 46.34°N, 334.16°E; Image No. HRL0000C5C2, 42.36°N, 343.87°E; Image No. FRT 00009BDC, 43.94°N, 313.205°E; Image No. HRL0000B2D5, 42.38°N, 317.20°E; Image No. FRT 0000A386, 41.62°N, 354.69°E; Image No. FRT 0000D3A1, 40.72°N, 332.58°E; Image No. FRT 000086E9, 42.18°N, 319.32°E; Image No. HRL0000D1B2, 40.30°N, 346.71°E.

more ferric iron than the plains (Allen et al., 2009; Amador et al., 2010). Similarly, in false color, visible–near-infrared browse products for ferrous and ferric iron minerals (VNIR-FEM, provided by NASA/Johns Hopkins University Applied Physics Laboratory), the mounds are commonly more green or red than the background plains (Fig. 13B); this suggests that the mounds may have more coatings or greater content of crystalline ferric oxides than the plains and that the plains may have greater content or larger particle size of iron minerals, especially olivine and pyroxene (CRISM Data Products website: http://crism-map.jhuapl.edu/popvnir.php). No spectral evidence was detected for evaporites, phyllosilicates, or hydrated sulfates.

5. Alternative hypotheses for the origin of the Acidalia mounds

Potential analogs for various types of mounds in the lowlands include features related to impact, ice (pingos or ice-disintegration features such as kames), sublimation, evaporation, magmatic eruption (lava volcanoes, pseudocraters, cinder cones, or tuff cones), springs, and mud volcanoes. These analogs have been discussed by numerous authors (Lucchitta, 1981; Rossbacher and Judson, 1981; Frey and Jarosewich, 1982; Carr, 1986; Grizzaffi and Schultz, 1989; Scott and Underwood, 1991; Kargel and Strom, 1992; Scott et al., 1995; Tanaka, 1997; Tanaka et al., 2003, 2005; Farrand et al., 2005; McGowan, 2009), and a review of interpretations was provided by Tanaka et al. (2005).

Briefly, in the 1980s and early 1990s, mounds associated with the concentric, arcuate ridges of the "thumbprint terrain" were interpreted from Viking data as pseudocraters, which can result from steam explosions when hot lava crosses wet surfaces such as lakes or ponds (Frey and Jarosewich, 1982; Carr, 1986). More recent studies, based on MOC, MOLA, and THEMIS IR data, looked at details of the geomorphology as well as geological relationships; these concluded that compelling evidence for volcanic or ice-related features was lacking and that the analogy most consistent with all the data would be a process similar to mud volcanism or mud volcanism with evaporite deposition around geysers and/or springs (Tanaka, 1997; Tanaka et al., 2003, 2005; Farrand et al., 2005; Rodríguez et al., 2007; McGowan, 2009).

Our work adds observations from HiRISE, CRISM, and regional mapping to the discussion of potential analogs. Below we consider salient arguments related to potential analogs, incorporating these new data.

5.1. Analogs other than mud volcanoes

5.1.1. Impact structures

The mounds clearly are not impact structures. None is associated with an ejecta blanket, and the variety of morphologies of the mounds is quite distinct from that of impact craters. The two mounds with heights measured by photogrammetry (above) have diameters of 750 and 650 m and maximum rim heights of approximately 180 m. This height is much greater than would be expected for impact craters with diameters from 650 to 750 m (Garvin et al., 2000) and such steep-sided mounds differ significantly in morphology from simple bowl-shaped impact craters. Finally, the

common alignment of the mounds at polygon boundaries and in arcuate ridges would seem to eliminate the possibility of an origin related to impacts, as impact processes would result in an irregular spatial distribution that would be unrelated to polygon boundaries or ridges.

5.1.2. Pingos

Similarly it is unlikely that the mounds are pingos. Pingos are ice-cored mounds on Earth that form in periglacial settings as a result of upward movement and freezing of groundwater. They commonly have fractures on their crests due to dilation of surface materials over expanding ice cores, and their surfaces are similar to that of the surrounding plains. The facts that the mounds in Acidalia have neither surface fractures nor albedo and texture similar to that of the plains, argues against the pingo analog. Farrand et al. (2005) also reached the conclusion that pingos are an unlikely analog for the Acidalia mounds, and this is consistent with a recent review of pingo-like features on Mars (Burr et al., 2009) and assessment of evidence for pingos from HiRISE data (Dundas and McEwen, 2010).

Our work provides support for a "non-pingo" analog, as an interpretation related to pingos is difficult to reconcile with HiRISE images showing the unfractured surfaces of the Acidalia mounds and their smooth textures and relatively high albedo which stand out against the knobby, rugose texture and generally lower albedo of the plains. In addition, CRISM results suggest that the Acidalia mounds and plains have different compositions, which would not be expected for pingos. Finally, there are several examples where mounds have been breached (e.g., Figs. 11A, B, and 12C), exposing their internal cores to the current martian atmosphere. If these mounds had been cored by ice, as in pingos, that ice would have been unstable in current martian conditions and would have sublimed, leaving collapse features. Since these mounds are intact and collapse features are not present, the pingo analog seems improbable.

5.1.3. Evaporite or spring-related features

Evaporite deposits are unlikely analogs in view of the high relief, moats, and flow-like structures of the mounds. Springs also seem like a weak analog, as a features created by springs would not explain the moats or flow-like structures of the mounds. Moreover, none of the hundreds of mounds studied in detail from HiRISE, MOC, and CTX images exhibited any evidence for the terracing or associated channel-like features that are common on terrestrial spring mounds and that have been described from possible examples of martian spring mounds in Arabia Terra (Allen and Oehler, 2008).

5.1.4. Magmatic features

Magmatic analogs seem unlikely, as lava is typically of lower albedo and higher thermal inertia than the mounds. However, tuff cones are not necessarily associated with surface lava. Tuff cones are structures built by explosive interaction between subsurface magma and groundwater (Wohletz and Sheridan, 1983). They are steep-sided and comprised of thickly bedded tephra. They commonly have single vents or craters near their centers. Farrand et al. (2005) addressed a tuff cone analog, and while their analysis favored a mud volcano type of origin, they noted that a tuff cone analog would not necessarily be inconsistent with the more cone-shaped mounds in Acidalia.

Our work provides additional argument against a tuff cone analog, as the range of morphologies of the mounds imaged with HiRISE is well beyond that associated with tuff cones. This range varies from surfaces that are smooth and unpitted to those with irregular pits; it also includes the moats, the broader domal morphologies, the near pancake shapes, and the examples of material apparently flowing from the mounds into polygon troughs and onto the plains. Lastly, since we have determined that there are tens of thousands of mounds in Acidalia that extend across the entire southern portion of this ~3000 km-diameter basin, a tuff cone analog would seem to require the presence of an enormous magmatic body in the shallow subsurface of Acidalia. Yet there is no evidence for this. Amazonian-aged lavas have not been confirmed in Acidalia from geomorphology, and regional gravity data (while complex and subject to multiple interpretations) show intermediate to low values in Acidalia that are distinct from the marked gravity highs associated with the volcanic edifices in Tharsis, Alba Patera, and Elysium (Fig. 14).

5.2. Mud volcano analog

5.2.1. Terrestrial mud volcanoes

Mud volcanoes are mounds formed by upwardly mobile masses of fine-grained sediment that move through conduits in the subsurface, primarily due to overpressure and resultant buoyancy. Key references describing surface characteristics, structure, modes of formation, and association with methane of terrestrial mud volcanoes include the works Hovland et al. (1997), Guliyev and Feizullayev (1997), Kopf (2002), Deville et al. (2003), Milkov and Sassen (2003), Murton and Biggs (2003), Etiope et al. (2004), Stewart and Davies (2006), and Evans et al. (2008).

Mud volcanoes typically develop in subaqueous, basinal settings that experience rapid deposition and subsidence and where the rate of sediment loading exceeds the rate at which water in the sediments can escape (Kopf, 2002). The rapid sedimentation results in sediments that are undercompacted at depth and therefore overpressured with respect to surrounding strata. In fine-grained sediments, overpressure can be maintained for millions of years because fluid flow is impeded by the low permeability of such sediments. Undercompacted sediments are less dense (more buoyant) than surrounding strata, and this buoyancy leads to upward movement of the low-density sediment package. Upward mobility can additionally be "triggered" by events that enhance overpressure (Kopf, 2002) such as tectonic compression, hydrothermal pulses, hydrocarbon generation, or injection of gas through dissociation of clathrates (a good example of the latter being the mud volcanoes in Lake Baikal caused by gas hydrate dissociation; Van Rensbergen et al., 2002). Upward flow also can be facilitated if confining pressure is reduced or if zones of weakness (such as faults and fractures) are opened through uplift and unloading due to removal of overburden. Hydrothermal pulses, uplift, and loss of overburden have the additional potential to destabilize clathrates and the gas expelled by that process could add to the overpressure and flow upward with mud. Kopf (2002) quotes: "When internal pressure in a sediment exceeds confining pressure and strength of rock, hydraulic fracturing and fluid + shale intrusion in the overburden occurs. Tectonic relaxation or erosion cause decrease in confining pressure and may trigger break-outs and mud movement." Any of the above kinds of triggers may initiate rapid and extensive mud volcanism.

Figs. 4 and 5 illustrate a variety of mud volcanoes from Azerbaijan. These show large mountainous features with mud flows (Figs. 4A, B, and 5A) as well as relatively flat, pedestal-like edifices having high-albedo patches (Figs. 4C, E, F, and 5A, B, E) that are remnants of mud lakes. Diameters of the high-albedo patches are variable but commonly a few hundred meters; diameters of entire pedestals or mountainous mud volcano systems are commonly 1–2 km but can approach tens of kilometers in some of the larger systems. As noted, heights of terrestrial mud volcanoes above land range up to 600 m, though entire systems – from mud source in the subsurface to the crests of the structures – can reach several kilometers.

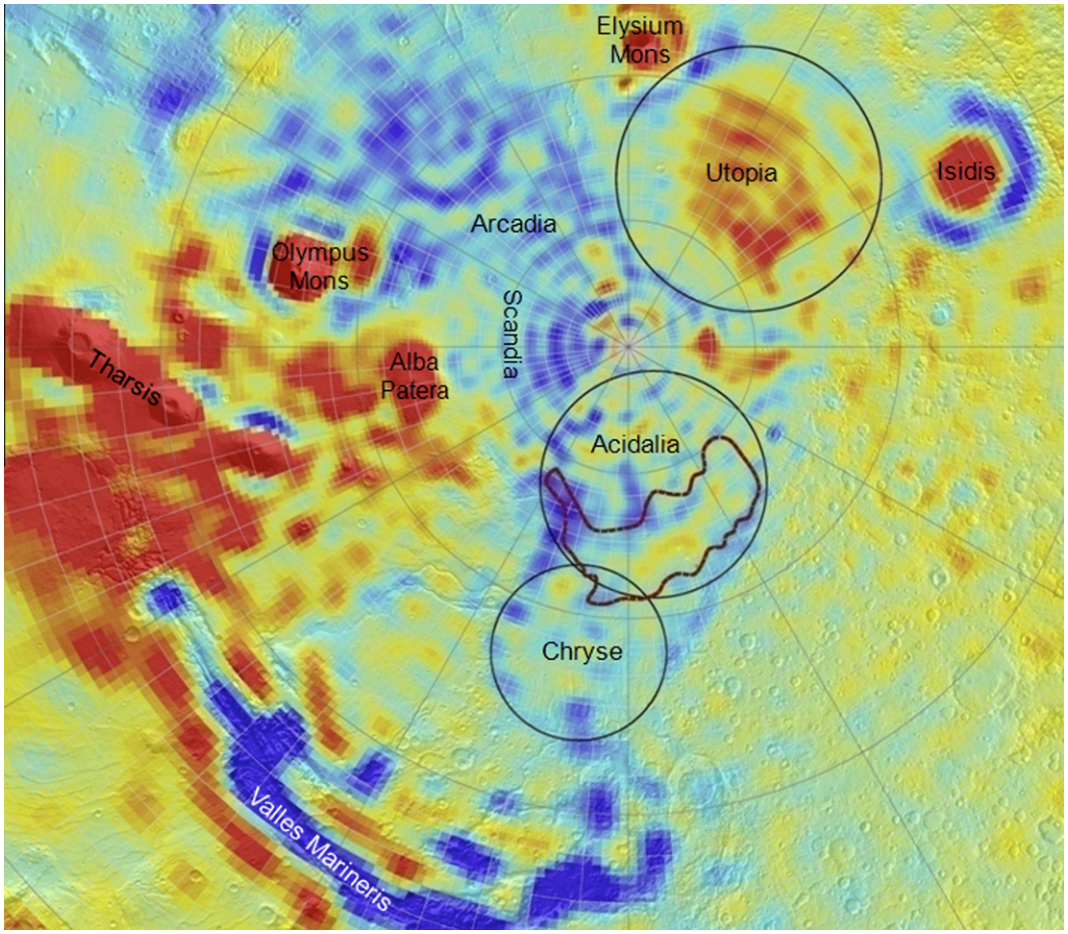

Fig. 14. Regional gravity. Data evaluated for the MGM1025 model provided in the MarsGIS DVD v. 1.4 and underlain by MOLA hillshade map with 128 pixels/degree. The values represented by the gravity map range from +2969 milligals (deep reds) to −486 milligals (dark blue). Approximate locations of quasi-circular depressions corresponding to the Chryse, Acidalia, and Utopia impact basins (Frey, 2006) are shown by black circles. Dark red outline within Acidalia is the "Generalized Area of Occurrence" of the mounds that have been mapped from Nighttime IR mosaic in the MarsGIS DVD.

The rock breccias brought to the surface during mud volcanism are often found in the extensive flows that form during active periods. Finer-grained muds accumulate during quiescent periods (Feyzullayev, personal communication, 2009), resulting in the crestal mud lakes; these mud lakes have relatively high albedo, reflecting accumulated salts, sulfates, carbonates, or various clays (Figs. 4F and 5E). Moats result from mud evacuation in the subsurface (Fig. 5B) (Evans et al., 2008). Concentric circular or ring-like features are common on the crests (Figs. 4E, F, and 5E), reflecting episodic formation and drying of mud lakes and/or faulting associated with the subsurface mud conduits. Aprons of finely textured, bright material can be deposited beyond the crests as a result of episodic, but relatively quiescent activity. Extended mud flows onto the plains are generally linear features with defined edges and distinctive textures (Fig. 4D). In contrast, some mud volcanoes, such as those reported from the Niger Delta, offshore Nigeria, have few flows associated with circular mounds; these are thought to arise from explosive eruptions dominated by gases and sediment (Graue, 2000).

Spatial density of mud volcanoes in an area of about 5000 km^2 in Azerbaijan converts to 20 mud volcanoes per 1000 km^2. In the most concentrated part of this area, the spatial density is approximately 40 per 1000 km^2. Because multiple high-albedo patches occur on many of the pedestals of the mud volcanoes in Azerbaijan, spatial density of these high-albedo patches would be 100+ features per 1000 km^2.

5.2.2. Acidalia mounds and the mud volcano analog

Many of the characteristics of the mounds in Acidalia have analogs in terrestrial mud volcanoes (Figs. 2, 3, 5C, D, 8, and 12) or are consistent with an interpretation of origin from a process similar to mud volcanism. These include

(1) diameters (Acidalia mounds: 300–2200 m, with an average of 830 m measured in this study; terrestrial mud volcanoes: diameters up to tens of kilometers but typically a few hundred meters to 2 km, Kopf, 2002);
(2) heights (Acidalia mounds: tens of meters to 180 m; terrestrial mud volcanoes: up to 600 m, Kopf, 2002);
(3) spatial density (Acidalia mounds: 21–114 mounds/1000 km^2 calculated in this study; terrestrial mud volcanoes: 20–40 mud volcanoes/1000 km^2 though density of the high-albedo patches on the pedestals of some of the mountain-forming mud volcanoes in Azerbaijan would be in the range of 100+/1000 km^2 (e.g., Fig. 4E and F) and one possibility is that some of the mounds in Acidalia may be comparable to these individual patches);
(4) sub-circular shapes;
(5) variable morphology (cones, domes, caldera-like features, and flat structures);
(6) smooth surface texture;
(7) relatively high albedo;
(8) aprons;

(9) pitted and non pitted crests;
(10) irregular to aligned clustering (alignment in terrestrial mud volcanoes typically follows faults, fractures, or structural highs);
(11) concentric circular crestal structures;
(12) moats;
(13) thermal inertia:

Apparent thermal inertia of the mounds is also consistent with a mud volcano analog. Extruded mud would be expected to have relatively low thermal inertia due to its fine grain size and semi-consolidated state (Putzig and Mellon, 2007). The mounds in this study are significantly darker than the surrounding plains in THEMIS nighttime IR images, implying that their thermal inertia is lower than that of the plains. Since Nighttime IR is only minimally affected by albedo and since mounds in Acidalia with both high and low albedo have dark responses in the Nighttime IR, it is likely that the dark responses in Nighttime IR reflect low thermal inertia, as has been suggested (Farrand et al., 2005).

Thermal inertia values calculated for a large region in Acidalia Planitia range from ~200 to 600 tiu, with local values (mainly to the north of the region in which we mapped the mounds) as high as 800 tiu (Putzig and Mellon, 2007). These values are characteristic of medium-to-coarse basaltic sand and gravel, or duricrust deposits, under martian atmospheric pressure (Martínez-Alonso et al., 2008). The estimates of thermal inertia for the mounds (190–240 tiu, Farrand et al., 2005) are characteristic of fine basaltic sand under martian surface conditions (Mellon et al., 2000). Erupted mud, when dry, might be partially indurated and have a higher thermal inertia than fine sand. However, following desiccation and many sequences of thermal cycling on the martian surface, that same mud could well shatter into sand-size fragments. Farrand et al. (2005) concluded that "The dried, loosely cemented, mud deposits would be a good match to both the albedo and thermal inertia measurements from the martian domes and cones."

(14) Mineralogy from CRISM:

CRISM results suggest subtle mineralogic differences between the mounds and the plains (Fig. 13), such that the mounds appear to have enhanced coatings or greater concentrations of ferric oxides than plains materials. Albedo alone is not likely to explain these differences, as some of the mounds, with albedos similar to that of the plains (e.g., CRISM image FRT 0000A386; Fig. 13A and B) still show the positive slopes in the VIS and reddish color in the VNIR-FEM image, suggesting enhanced coatings or ferric oxides. These results are consistent with mud volcanism, as in this process, materials extruded to the surface are derived from sediments making up the surrounding plains. The slight spectral differences suggestive of enhanced coatings or ferric minerals in the mounds would be consistent with alteration by water (Wyatt, 2008) as might be expected within fluidized, rising mud. These results are also consistent with recent studies of weathering of dolerite in the Antarctic (Chevrier et al., 2006) which showed that slow weathering under the cold and dry conditions of the Antarctic resulted in replacement of Fe^{2+} in pyroxene of the dolerite with Fe^{3+} in poorly crystalline ferric (oxy) hydroxides.

CRISM NIR data failed to show evidence of any well-formed minerals on the Acidalia mounds. This is in contrast to terrestrial mud volcanoes which commonly contain a mixture of clays (smectite, illite, kaolinite, and vermiculite), crusts with carbonates, gypsum, iron hydroxides, salts, and occasional occurrences of amorphous silica, sulfides, anhydrite or barite (Guliyev and Feizullayev, 1997; Kopf, 2002; Scholte et al., 2003; Deville, 2009; Etiope, personal communication, 2009). In addition, there is now CRISM evidence for Noachian phyllosilicates in Mawrth Vallis (Loizeau et al., 2010), and some of these phyllosilicates are likely to have washed into the Acidalia basin and been brought to the surface with mud volcanism.

Some of these types of minerals, if present in low concentrations on the Acidalia mounds, might not be detectable by the CRISM detector or from orbit. Certainly the cold martian temperatures during the Amazonian may have minimized authigenic clay formation in the mounds (Tosca, 2009), as surface temperatures below freezing would limit liquid water available for reaction with sediments (McAdam et al., 2004; Chevrier et al., 2006). Also, since Chevrier et al. (2006) have shown that weathering of dolerites in the Antarctic results formation of poorly crystalline Fe^{3+} minerals, it is possible that such minerals (perhaps in the coatings on the mounds indicated by CRISM) could obscure CRISM detection of other minerals or clays that might be present.

Moreover, the lack of CRISM mineral signatures from the mounds may be part of a larger, regional picture (Salvatore et al., 2010), since there is a similar lack of mineral signatures in CRISM data for plains materials in Acidalia – even though a basaltic plains composition is indicated by data from TES, OMEGA (Observatoire pour la Minéralogie, l'Eau, les Glaces, et l'Activité – the Visible and Infrared Mineralogical Mapping Spectrometer on Mars Express), and GRS (Gamma Ray Spectrometer on Mars Odyssey) (Wyatt and McSween, 2002; Wyatt, 2008). So, although olivine or pyroxene might be expected in the basaltic plains of Acidalia, they are, in general, not detected with CRISM. In fact, the muted mafic signatures in Acidalia are particularly evident in sediments mapped as Vastitas Borealis units, and it has been speculated that cryoturbation and other processes may have modified mafic signatures in the region (Salvatore et al., 2009, 2010). It may be, therefore, that both the mounds and plains of Acidalia contain minerals that are undetected by CRISM.

In summary, we cannot be certain that clays would have formed in the cold temperatures that were likely when the Acidalia mounds were formed. Although clays are not absolutely necessary for mud volcanism, the data identifying Noachian phyllosilicates in Mawrth Vallis, suggest the possibility that clayey phyllosilicates may have washed into Acidalia from Highlands' sources. The plasticity and fine grain size of such clays may have facilitated the process of mud volcanism. However, if clays from any source were present in relatively low concentrations or were coated by poorly crystalline alteration products that formed on the mounds, they may not be detectable from orbit.

At a minimum, the CRISM results suggesting enhanced coatings or concentrations of ferric minerals in the mounds would support an interpretation of mound-formation through a process involving fluid and sediment interaction, and this would be consistent with a process similar to terrestrial mud volcanism.

(15) Geologic setting:

Perhaps most significantly, the unique geologic setting of Acidalia supports the analog of mud volcanism, as extensive mud volcanism would be predicted from the geologic history of the region.

The critical ingredients for mud volcanism are rapid, subaqueous deposition of thick sequences of fine-grained sediments and development of overpressure (Kopf, 2002; Deville et al., 2003). The Chryse–Acidalia area clearly received large amounts of sediment and fluid from the Hesperian outflows (Rice and Edgett, 1997; Tanaka et al., 2005). Head et al. (1999) estimated that an average of 600 m of sediment and effluent was deposited by the outflow channels, and Tanaka et al. (2003) noted that the relative paucity of "ghost craters" in the Acidalia area might reflect accumulation of sediments thick enough to bury most of those craters.

Certainly, accumulation of substantial thicknesses of outflow sediments in Acidalia would have been fostered by the combina-

tion of the embayment-like geometry of the Chryse–Acidalia region, trapping in the proposed (Frey, 2006) impact basin (Fig. 1), and by the potential spillover and from Chryse to Acidalia. Because of these relationships, Acidalia is likely to have been a depocenter for thick accumulations of rapidly-deposited sediments from the Hesperian outflows. Furthermore, the proximal setting of Chryse with respect to the outflows would likely result in its having trapped the coarse-grained fraction of outflow sediments. This would leave the finer-grained sediments to be concentrated in the distal and deeper, Acidalia portion of the embayment. The rapid deposition and concentration of fines in Acidalia would make it the ideal location for development of overpressure and mud volcanism.

In summary, the combined morphological, physical, mineralogical, and regional geologic data support an origin for the mounds in Acidalia from a sedimentary process most compatible with a mud volcano analog.

6. Mud volcanism in Acidalia

6.1. Distinctive martian attributes

Despite the similarities to terrestrial mud volcanoes, mud volcanism in Acidalia is likely to have had uniquely martian attributes. While terrestrial mud volcanism is commonly initiated (triggered) by tectonic compression or hydrocarbon generation (Kopf, 2002), neither of these processes has been described in Acidalia. Nevertheless, a variety of initiating mechanisms have been proposed for mud volcanism in different parts of the martian lowlands. These include (1) dewatering of pressurized zones in the Simud/Tiu debris flow giving rise to flat mud-volcano-like features in Chryse Planitia (Tanaka, 1999); (2) impact-related, seismically-induced liquifaction and shoaling of unconsolidated Vastitas Borealis sediments in the highland-lowland boundary area of Utopia (Skinner et al., 2008); (3) rapid sedimentation with corresponding compaction and devolatilization in Acidalia, Chryse, and Isidis (Skinner and Mazzini, 2009); and (4) sublimation of a cold-based glacier or destabilization of methane- or CO_2-clathrates for pitted cones in the region of giant polygons in Cydonia Mensae/southern Acidalia (McGowan, 2009).

The basinwide occurrence of the mounds in Acidalia may suggest triggering mechanisms, not unlike those already proposed, but having a more regional scope. Rapid sedimentation alone (and the resultant build-up of overpressure with compaction) might account for basinwide mud volcanism, but terrestrial analogs suggest that this is a relatively slow process compared with mud volcanism initiated by additional driving forces (Kopf, 2002). Given the correspondence of the Acidalia mounds to Vastitas Borealis units (which some consider to be paleo-ocean deposits; Tanaka et al., 2005), consideration also should be given to sublimation of a major body of water such as a frozen ocean (Tanaka and Banerdt, 2000; Kreslavsky and Head, 2002; Kargel, 2004; Dohm et al., 2009) and tectonic rebound associated with that sublimation. These processes remove overburden and thereby reduce confining pressure. This, in turn, increases relative overpressure of sediments at depth. Hydrothermal or compressive pulses from Tharsis could similarly be potential regional triggers that would increase overpressure at depth. Finally, the global hydrologic model of Andrews-Hanna et al. (2007) suggests that the lowlands may have had upwelling of groundwater due to shallow depths to the water table, and this upwelling may have enhanced the potential for overpressure in Acidalia. Thus, overpressure development in Acidalia may have been favored by the rapid deposition of thick, fine-grained sediments in the Acidalia Basin coupled with thermal pulses from Tharsis, sublimation, and upwelling of groundwaters (see also discussions in Hanna and Phillips (2005)). If volatiles such as carbon dioxide or methane were trapped as clathrates in ocean-bottom sediments or in permafrost within Acidalia (Kargel, 2004; Max and Clifford, 2004; McMenamin and McGill, 2007; Clifford et al., 2009; Clifford et al., in press), hydrothermal pulses from Tharsis or loss of overburden could have destabilized those clathrates, by increasing subsurface temperatures or reducing confining pressures, respectively. Such destabilization would have released gas basinwide, adding to the overpressure, and that, in turn, could have provided an additional trigger for mud volcanism on a regional scale. It has also been noted that extensive lenses of clathrates might "self-dissociate" because of their low thermal conductivities and resultant potential warming of underlying sediments (McGowan, 2009). This process, too, could have been part of a combination of triggering events that initiated mud volcanism over the entire region of southern Acidalia.

The abundance of mud flows expected on a martian plain also may be distinctive. Many mud volcanoes on Earth (such as those in Azerbaijan) have large, overlapping flows of mud (Figs. 4A, B, and 5) which can be traced for kilometers. We have seen few comparable features on Mars. While there is evidence of limited flow from some of the Acidalia mounds (Figs. 9 and 10), most mounds appear as simple circular structures.

The lack of extensive mud flows in Acidalia might be related to martian mud extrusion rates, sediment to water or gas ratios, viscosity, density, or grain size, as these factors influence morphology and extent of flow in terrestrial mud volcanoes (Judd and Hovland, 2007). In this regard, the Acidalia mounds may find analogy in the mud volcanoes that form in deltaic settings, like those in the offshore Niger Delta, where explosive exhalations of gas and sediment result in typically circular mounds lacking flows onto the plains (Graue, 2000). Moreover, the low Amazonian temperatures might have minimized the potential for flow by relatively rapid freezing of erupting martian muds. Thus, the circular Acidalia mounds that appear to be covered by a thin veneer of smooth material might represent cases where the low temperatures and/or specific mud characteristics impeded all flow away from the mounds. Other mounds that are associated with the flow-like features might represent cases where mud volcanism brought up slurries that were warm enough to have produced limited flow. In some instances, mud lobes that might have formed in Acidalia may have spread out over the plains forming relatively thin sheets. Precipitation of minerals and consequent induration of these may have been limited compared to the mounds themselves, due to the potentially large area over which such sheets may have been deposited and resultant dilution of mineral concentrations. In terrestrial mud volcanoes, flows onto the plains can form sheet-like structures, (e.g., Fig. 4D) and some of the oldest and most eroded flows blend into the landscape and are difficult to discern. This may be the case in Acidalia as well, as there are several instances of indistinct flow-like features extending from mounds (Fig. 5C and D). It is possible, therefore, that mud flow in Acidalia was limited by a combination of cold Amazonian temperatures and distinctive physical properties of martian mud slurries. At the same time, the plains of Acidalia may be crossed by some remnants of thin mud flows that are simply difficult to recognize.

6.2. Flow in Acidalia Mensa

The Acidalia Mensa platform (Fig. 1) includes the Vastitas Borealis Marginal Unit, as well as the Noachian Nepenthes Mensae and Noachis Terra Units. These are embayed by the Vastitas Borealis Interior Unit, suggesting that Acidalia Mensa was a long-term, high-standing structure or was uplifted prior to the Early Amazonian. The mounds in Acidalia Mensa overlie all of these units, though it is the Noachis Terra Unit that includes regions where,

because materials of the mounds and that filling the troughs appear to be the same, the possibility exists that mud may have flowed from the mounds to the troughs and surrounding areas (Fig. 11). If this were the case, then fracturing associated with the Noachis Terra Unit might have provided zones of weakness through which volatiles or warm waters may have ascended, promoting a form of mud volcanism on this platform. This possibility would be consistent with the suggestion by Tanaka et al. (2003) that uplift of this platform may have involved upwelling of volatiles.

6.3. Flow at polygon boundaries

Many of the mounds in Acidalia occur at polygon boundaries, suggesting a relationship between the two. These mounds commonly occur in the troughs between polygons or at the edges of the polygons, immediately adjacent to the troughs. This has also been observed by McGowan (2009). The mounds in the troughs are usually intact and show little physical disturbance related to the formation of the troughs (Figs. 2 and 12A, B), as if the mounds were younger than the troughs. Therefore, it is possible the formation of mounds at or near the edges of polygons might be related to upward flow along zones of weakness created by the earlier formation of the polygons.

6.4. Potential venting of gas to the martian atmosphere

Mud volcanism on Earth vents major quantities of gas (mainly methane) and has been estimated to contribute about ~25% of the ~40–45 $\times 10^6$ tons/year of methane released to the atmosphere each year by geological sources (which include macro- and micro-seeps, gas hydrates, magmatic and geothermal sources, mid-ocean ridges, and mud volcanoes; Hovland et al., 1997; Etiope and Klusman, 2002; Kopf, 2002; Etiope et al., 2004, 2010; Kvenvolden and Rogers, 2005; Etiope and Ciccioli, 2009).

On Mars, it has been suggested that significant amounts of methane (from either non-biological or biological sources) may exist in the subsurface as free gas and gas hydrates (Max and Clifford, 2000, 2001; Pellenbarg et al., 2003). Calculations suggest that the methane hydrate stability zone (HSZ) on Mars could extend from depths of 15 m to ~12–22 km, depending on the value of mean global heat flow (currently estimated at ~15–30 mW/m^2; Clifford et al., 2009; Clifford et al., in press). This zone overlaps with the depths likely to be affected by mud volcanism. Thus, it is possible that profuse mud volcanism in Acidalia may have released significant quantities of gas to the martian atmosphere if the eruptive process were triggered by, or caused, destabilization of gas hydrates. If this occurred, then the martian climate may have been affected, as may have happened on Earth during past episodes of massive clathrate destabilization (Kvenvolden and Rogers, 2005).

6.5. Uniqueness of Acidalia, habitability, and astrobiological potential

While potential mud volcanism has been reported from numerous areas in the martian lowlands (references listed in the Introduction), Acidalia stands out in two respects: It has a massive number of these mounds (tens of thousands, at least) and the mounds are distributed across the entire southern portion of the proposed ~3000 km impact basin. In most of the other lowland regions with possible mud volcanoes, the mud volcano-like features are limited areally and/or in numbers. Moreover, some of these possible mud volcanoes may actually be more analogous to other types of domed structures. For example, some of the mounds in Utopia are seen in HiRISE images to have fractured surfaces and seem potentially comparable to pingos (Dundas et al., 2008; Burr et al., 2009; but see also De Pablo and Komatsu, 2009; Dundas and McEwen, 2010). Other mounds in Utopia have been likened to mud volcanoes but these have been suggested to result from accumulation of impact ejecta between annular rings of the Utopia multi-ring structure, with pitted cones being possible relics of impact-related liquefaction of unconsolidated materials (Skinner and Tanaka, 2007; Skinner et al., 2008). Mounds interpreted as mud volcanoes at the intersection of the Isidis/Utopia ringed basins may reflect enhanced fracturing at the point of overlap (McGowan and McGill, 2010). However, compared to the mounds in Acidalia, the Utopia and Isidis features are present in significantly smaller numbers and are restricted to portions of each basin. Another example is the pitted knobs in Chryse Planitia that have been compared to mud volcanoes or cinder cones (Rodríguez et al., 2007). Only small numbers of these have been reported, and though Chryse most likely received the coarser sediments deposited by outflow sedimentation, it would not be surprising if a few localities contained enough mud to foster some form of mud volcanism. Thus, while forms of mud volcanism may have occurred in Utopia, Isidis, and Chryse as well as in Acidalia, it is only the mud volcano-like features in Acidalia that seem occur over a great portion of the entire basin rather than at its periphery, and it is likely that the sedimentary input, fluid content, triggers, and timing of events in the four regions may have been different.

What appears to be distinctive in Acidalia are the large number of mounds and their basinwide distribution. These characteristics are likely to reflect the fact that Acidalia was the primary depocenter for the fine fraction of the sediments deposited by the Hesperian outflows. No other part of the lowlands is situated to have received such a large portion of fines from the outflow floods. This is what distinguishes Acidalia from other parts of the martian lowlands. Acidalia's geologic setting may additionally endow this basin with unique characteristics from an astrobiological perspective. The Chryse–Acidalia embayment has an exceptionally large catchment area that would have drained a substantial portion of the southern highlands (Oehler and Allen, 2009). If microbial life developed on Mars and survived in highlands regions that drained into Chryse–Acidalia, runoff from that area could have entrained microbial biosignatures of the life forms from that watershed. Because organic materials tend to accumulate and be preserved with the fine-grained fraction of sediments (Schieber, 2003; Potter et al., 2005), organic remnants of possible martian life in Acidalia's watershed would have been deposited with the fine-grained sediments and fluids that were concentrated in Acidalia because of its distal position. Moreover, the abundance of fine-grained sediments in Acidalia could have protected any deposited organics from oxidation or exposure to radiation, thereby enhancing their preservation potential in that basin. Such preserved materials could include morphological microfossils, chemical degradation products of biomolecules from past life from the highlands catchment area, or mineralogical biosignatures.

There is the additional possibility that the subsurface in Acidalia could have supported indigenous microbial life. On Earth, microbial assemblages have been found in the subsurface of mud volcano systems of the Gulf of Mexico, supported by the upwelling of hot fluids containing abundant dissolved organic matter (Joye et al., 2009).

Recent hydrological modeling suggests that upwelling of groundwaters may have occurred in parts of the lowlands including Acidalia due to a combination of shallow depth of the water table and regional slope (Andrews-Hanna et al., 2007). The profusion of mud volcano-like mounds in Acidalia may have been enhanced by this process. In addition, such upwelling groundwaters may have been channeled to the surface through the conduits created by the extensive mud volcanism, as such conduits can provide long-lived pathways for water and gas migration and release (Etiope et al., 2010). Since upwelling waters could have contained

dissolved organics derived from Hesperian or Noachian strata and additionally may have provided warmth on an increasingly cold planet, subsurface accumulation of these waters may have provided microhabitats in Acidalia that could have supported *in situ* microbial populations. Such microhabitats may even support an endolithic microbiota of extant organisms.

Thus, ingredients for habitability might have been well established in Acidalia: a fluid-rich subsurface potentially containing abundant organic nutrients. Moreover, mud volcanism may have brought minimally-altered samples to the surface from such habitable zones at depth. It is because Acidalia is ideal for development of mud volcanism coupled with its potential to hold astrobiologically-important deposits that we believe the mounds in this region could be important sites for future sample collection and analysis.

7. Conclusions

Tens of thousands of high-albedo mounds occur across the southern part of the Acidalia impact basin. These structures have geologic, physical, mineralogic, and morphologic characteristics consistent with an origin from a sedimentary process similar to terrestrial mud volcanism. On Mars, this process will have had distinctive attributes due to the climatic history of the planet. We propose that the profusion of mounds in Acidalia is a consequence of this basin's unique geologic setting, being the depocenter for the fine fraction of sediments delivered by the outflow channels from the highlands. This setting is ideal for accumulation of mud and fluid and for the development of sedimentary overpressure. The immense number of these mounds, coupled with their widespread distribution, may additionally reflect a basinwide event that triggered eruption over the entire region. Examples of such events might include loss of overburden through sublimation of a frozen body of water and tectonic readjustment to that sublimation, dissociation of gas hydrates, hydrothermal/tectonic pulses from Tharsis – or any combination thereof. Significant releases of gas may have resulted from the extensive mud volcanism. Long-lived, potentially habitable environments may have been established by the accumulation of regionally upwelling groundwaters in the conduits created by the proposed mud volcanism.

Mud volcanism provides a mechanism for transporting sediments from relatively great depth to the surface in minimally-altered form. Such sediments may be of astrobiological significance, as they could contain chemical biomarkers, mineral biosignatures, or structural remains from past life deposited from Acidalia's large watershed or from indigenous, endolithic microorganisms (either past or present) that may have thrived in porous, fluid-rich microhabitats in the subsurface. None of the previous landings on Mars was located in an area with features identified as potential mud volcanoes. Thus we propose that the mounds in Acidalia may offer a new class of exploration target for Mars.

Acknowledgments

We thank NASA and the Astromaterials Research and Exploration Science Directorate at the Johnson Space Center (JSC) for facilities and support. We are especially grateful to Drs. G. Etiope (Istituto Nazionale di Geofisica e Vulcanologia, Rome, Italy) and A. Feyzullayev (Azerbaijan National Academy of Sciences, Baku) for their insights into processes of terrestrial mud volcanism, to Dr. S.M. Clifford (Lunar and Planetary Institute, Houston) for discussions of clathrates on Mars and review of portions of the manuscript dealing with potential venting of methane from hydrates, to Dr. J. Dohm (University of Arizona) for discussions regarding a potential martian ocean, and to Mr. M. Salvatore and Ms. L. Roach (both of Brown University, Providence, RI) for analyses of CRISM scene HRL00003837. Mr. O. Thomas and Mr. D. Bretz (Image Science and Analysis Laboratory at JSC) provided photogrammetric estimates of relief of domes in HiRISE stereo pairs. Dr. W. Farrand (Space Science Institute, Boulder, CO) read an early version of the paper and provided excellent suggestions. Mapping of individual mounds in Acidalia was carried out by Mr. David Baker (St. Lawrence University, NY) and Ms. Elena Amador (University of California, Santa Cruz) during their summer 2008 and 2009 Lunar and Planetary Institute Internships. Ms. Amador also provided analyses of additional CRISM images that covered areas in Acidalia having mounds. We are also grateful to two anonymous reviewers for many suggestions which have significantly improved this manuscript. We thank the CRISM, HiRISE, MOC, and THEMIS teams for providing image data used in this study and Google Earth for permission to use their images.

References

Allen, C.C., 1979. Volcano/ice interactions on Mars. J. Geophys. Res. 84, 8048–8059.
Allen, C.C., Oehler, D.Z., 2008. A case for ancient springs in Arabia Terra, Mars. Astrobiology 8 (6), 1093–1112.
Allen, C.C., Oehler, D.Z., Baker, D.M., 2009. Mud volcanoes – A new class of sites for geological and astrobiological exploration of Mars. Lunar Planet. Sci. XXXX. Abstract 1749.
Amador, E.S., Allen, C.C., Oehler, D.Z., 2010. Regional mapping and spectral analysis of mounds in Acidalia Planitia, Mars. Lunar Planet. Sci. XXXXI. Abstract 1037.
Andrews-Hanna, J.C., Phillips, R.J., Zuber, M.T., 2007. Meridiani Planum and the global hydrology of Mars. Nature 446, 163–166.
Andrews-Hanna, J.C., Zuber, M.T., Banerdt, W.B., 2008. The Borealis basin and the origin of the martian crustal dichotomy. Nature 453, 1212–1215.
Baker, V.R., Strom, R.G., Gulick, V.C., Kargel, J.S., Komatsu, G., Kale, V.S., 1991. Ancient oceans, ice sheets, and the hydrological cycle of Mars. Nature 352, 589–594.
Burr, D.M., Tanaka, K.L., Yoshikawa, K., 2009. Pingos on Earth and Mars. Planet. Space Sci. 57, 541–555.
Carr, M.H., 1986. Mars – A water-rich planet? Icarus 68, 187–216.
Chevrier, V., Mathé, P.–E., Gunnlaugsson, H.P., 2006. Magnetic study of an Antarctic weathering profile on basalt: Implications for recent weathering on Mars. Earth Planet. Sci. Lett. 244 (3–4), 501–514.
Christensen, P.R., 2003. Formation of recent martian gullies through melting of extensive water-rich snow deposits. Nature 322, 45–48.
Clifford, S.M., Heggy, E., Boisson, J., McGovern, P., Max, M.D., 2009. The occurrence and depth of subpermafrost groundwater on present-day Mars: Implications of revised estimates of crustal heat flow, thermal conductivity, and freezing point depression. Lunar Planet. Sci. XXXX. Abstract 2557.
Clifford, S.M., Lasue, J., Heggy, E., Boisson, J., McGovern P., Max, M.D., in press. The depth of the martian cryosphere: Revised estimates and implications for the existence and detection of subpermafrost groundwater. J. Geophys. Res.
Davis, P.A., Tanaka, K.L., 1995. Curvilinear ridges in Isidis Planitia, Mars – The result of mud volcanism? Lunar Planet. Sci. XXIV, 321–322.
De Pablo, M.A., Komatsu, G., 2009. Possible pingo fields in the Utopia basin, Mars: Geological and climatical implications. Icarus 199, 49–74.
Deville, E., 2009. Mud volcano systems. In: Lewis, Neil, Moretti, Antonio (Eds.), Volcanoes: Formation, Eruptions and Modelling. Nova Science Publishers, pp. 95–125.
Deville, E., Battani, A., Griboulard, R., Guerlais, S., Herbin, J.P., Houzay, J.P., Muller, C., Prinzhofer, A., 2003. The origin and process of mud volcanism: New insights from Trinidad. In: Van Rensbergen, P., Hillis, R.R., Maltman, A.J., Morley, C.K. (Eds.), Subsurface Sediment Mobilization, vol. 216. Geological Society, London, Spec. Publ., pp. 475–490.
Dohm, J.M., and 20 colleagues, 2009. GRS evidence and the possibility of paleooceans on Mars. Planet. Space Sci. 57, 664–684.
Dundas, C.M., McEwen, A.S., 2010. An assessment of evidence for pingos on Mars using HiRISE. Icarus 205, 244–258.
Dundas, C.M., Mellon, M.T., McEwen, A.S., Lefort, A., Keszthelyi, L.P., Thomas, N., 2008. HiRISE observations of fractured mounds: Possible martian pingos. Geophys. Res. Lett. 35, L04201. doi:10.1029/2007GL031798.
Etiope, G., Ciccioli, P., 2009. Earth's degassing: A missing ethane and propane source. Science 323, 478.
Etiope, G., Klusman, R.W., 2002. Geologic emissions of methane to the atmosphere. Chemosphere 49, 777–789.
Etiope, G., Feyzullayev, A., Baciu, C.L., Milkov, A.V., 2004. Methane emission from mud volcanoes in eastern Azerbaijan. Geology 32 (6), 465–468.
Etiope, G., Oehler, D.Z., Allen, C.C., 2010. Methane emissions from Earth's degassing: Implications for Mars. Planet. Space Sci., submitted for publication.
Evans, R.J., Davids, R.J., Steward, S.A., 2007. Internal structure and eruptive history of a kilometer-scale mud volcano system, South Caspian Sea. Basin Res. 19 (1), 153–163.
Evans, R.J., Stewart, S.A., Davies, R.J., 2008. The structure and formation of mud volcano summit calderas. J. Geol. Soc. 165, 769–780.

Farrand, W.H., Gaddis, L.R., Keszthlyi, L., 2005. Pitted cones and domes on Mars: Observations in Acidalia Planitia and Cydonia Mensae using MOC, THEMIS, and TES data. J. Geophys. Res. 110. doi:10.1029/2004JE002297.
Frey, H.V., 2006. Impact constraints on, and a chronology for, major events in early Mars history. J. Geophys. Res. 111, E08S91. doi:10.1029/2005JE002449.
Frey, H., 2008. Ages of very large impact basins on Mars: Implications for the late heavy bombardment in the inner Solar System. Geophy. Res. Lett. 35, L13203. doi:10.1029/2008GL033515.
Frey, H., Jarosewich, M., 1982. Subkilometer martian volcanoes – Properties and possible terrestrial analogs. J. Geophys. Res. 87, 9867–9879.
Frey, H., Lowry, B.L., Chase, S.A., 1979. Pseudocraters on Mars. J. Geophys. Res. 84, 8075–8086.
Garvin, J.B., Frawley, J.J., Sakimoto, S.E.H., Schnetzler, C., 2000. Global geometric properties of martian impact craters: An assessment from Mars Orbiter Laser Altimeter (MOLA) digital elevation models. Lunar Planet. Sci. XXXI. Abstract 1619.
Golombek, M.P., Edgett, K.S., Rice Jr., J.W. (Eds.), 1995a. Mars Pathfinder Landing Site Workshop II: Characteristics of the Ares Vallis region and field trips in the channeled Scabland, Washington, LPI Tech. Rep. 95-01, Part 1, 63 pp.
Golombek, M.P., Edgett, K.S., Rice Jr., J.W. (Eds.), 1995b. Mars Pathfinder Landing Site Workshop II: Characteristics of the Ares Vallis region and field trips in the channeled Scabland, Washington, LPI Tech. Rep. 95-01, Part 2, 47 pp.
Graue, K., 2000. Mud volcanoes in deepwater Nigeria. Marine Petrol. Geol. 17, 959–974.
Grizzaffi, P., Schultz, P.H., 1989. Isidis basin – Site of ancient volatile-rich debris layer. Icarus 77, 358–381.
Guliyev, I.S., Feizullayev, A.A., 1997. All about mud volcanoes. In: Monograph, Geology Institute, Azerbaijan National Academy of Sciences. Baku Publishing House, NAFTA-PRESS, 52 p.
Hanna, J.C., Phillips, R.J., 2005. Hydrological modeling of the martian crust with application to the pressurization of aquifers. J. Geophys. Res. 110, E01004. doi:10.1029/2004JE002330.
Hartmann, W.K., 2005. Martian cratering 8: Isochron refinement and the chronology of Mars. Icarus 174, 294–320.
Hartmann, W.K., Neukum, G., 2001. Cratering chronology and the evolution of Mars. Space Sci. Rev. 96, 165–194.
Head, J.W., Hiesinger, H., Ivanov, M.A., Kreslavsky, M.A., Pratt, S., Thomson, B., 1999. Possible ancient oceans on Mars: Evidence from Mars Orbiter Laser Altimeter data. Science 286, 2134–2137.
Hovland, M., Hill, A., Stokes, D., 1997. The structure and geomorphology of the Dashgil mud volcano, Azerbaijan. Geomorphology 21, 1–15.
Joye, S.B., and 10 colleagues, 2009. Metabolic variability in seafloor brines revealed by carbon and sulphur dynamics. Nat. Geosci. 3. doi:10.1038/NGEO475.
Judd, A., Hovland, M., 2007. Seabed Fluid Flow. Cambridge University Press. 475 pp.
Kargel, J.S., 2004. Mars: A Warmer Wetter Planet. Proxis-Springer. 557 p.
Kargel, J.S., Strom, R.G., 1992. Ancient glaciation on Mars. Geology 20, 3–7.
Kite, E.S., Hovius, N., Hillier, J.K., Besserer, J., 2007. Candidate mud volcanoes in the Northern Plains of Mars. American Geophysical Union, Fall Meeting 2007 (abstract #V13B-1346).
Kopf, A.J., 2002. Significance of mud volcanism. Rev. Geophys. 40 (2), 2–52.
Kreslavsky, M.A., Head III, J.W., 2002. Fate of outflow channel effluents I the northern lowlands of Mars – The Vastitas Borealis Formation as a sublimation residue from frozen ponded bodies of water. J. Geophys. Res. 107, E12 4-1–E12 4-25. Doc. No. 5121. doi:10.1029/2001JE001831.
Kvenvolden, K.A., Rogers, B.W., 2005. Gaia's breath – Global methane exhalations. Marine Petrol. Geol. 22, 579–590.
Loizeau, D., Mangold, N., Poulet, F., Ansan, V., Hauber, E., Bibring, J.-P., Gondet, B., Langevin, Y., Masson, P., Neukum, G., 2010. Stratigraphy in the Mawrth Vallis region through OMEGA, HRSC color imagery and DTM. Icarus 205, 396–418.
Lucchitta, B.K., 1981. Mars and Earth – Comparison of cold-climate features. Icarus 45, 264–303.
Marinova, M.M., Aharonson, O., Asphaug, E., 2008. Mega-impact formation of the Mars hemispheric dichotomy. Nature 453, 1216–1219.
Martínez-Alonso, S., Mellon. M.T., Rafkin, S.C.R., Zurek, R.W., McEwen, A.S., Putzig, N.E., Searls, M.L., and the HiRISE Team, 2008. HiRISE characterization of thermophysical units at Acidalia Planitia, Mars. Lunar Planet. Sci. XXXIX. Abstract 2266.
Max, M.D., Clifford, S.M., 2000. The state, potential distribution, and biological implications of methane in the martian crust. J. Geophys. Res. 105 (E2), 4165–4171.
Max, M.D., Clifford, S.M., 2001. Initiation of martian outflow channels: Related to the dissociation of gas hydrate? Geophys. Res. Lett. 28 (9), 1787–1790.
Max, M.D., Clifford, S.M., 2004. The origin and distribution of methane hydrate in the martian crust. In: Second Conference on Early Mars. Abstract 8083.
McAdam, A.C., Leshin, L.A., Harvey, R.P., Hoffman, E.J., 2004. Antarctic soil derived from the Ferrar Dolerite and implications for the formation of martian surface materials. In: Second Conference on Early Mars. Abstract 8050.
McEwen, A.S., Preblich, B.S., Turtle, E.P., Artemieva, N.A., Golombek, M.P., Hurst, M., Kirk, R.L., Burr, D.M., Christensen, P.R., 2005. The rayed crater Zunil and interpretations of small impact craters on Mars. Icarus 176, 351–381.
McGowan, E., 2009. Spatial distribution of putative water related features in southern Acidalia/Cydonia Mensae, Mars. Icarus 202, 78–89.
McGowan, E.M., McGill, G.E., 2010. The Utopia/Isidis overlap; Possible conduit for mud volcanism. Lunar Planet. Sci. 41. Abstract 1070.
McMenamin, D.S., McGill, G.E., 2007. Martian glacial morphology, geomorphology, and atmospheric methane. Lunar Planet. Sci. XXXVIII. Abstract 1161.
Mellon, M.T., Jakosky, B., Kieffer, H., Christensen, P., 2000. High resolution thermal inertia mapping from the Mars Global Surveyor Thermal Emission spectrometer. Icarus 148, 437–455.
Mellon, M.T., Kretke, K.A., Smith, M.D., Pelkey, S.M., 2002. A global map of thermal inertia from Mars Global Surveyor mapping-mission. Lunar Planet. Sci. XXXIII. Abstract 1416.
Milkov, A.V., Sassen, R., 2003. Global distribution and significance of mud volcanoes. In: AAPG Annual Convention, Salt Lake City, Utah, May 11–14 (abstract).
Murton, B.M., Biggs, J., 2003. Numerical modeling of mud volcanoes and their flows using constraints from the Gulf of Cadiz. Marine Geol. 195, 223–236.
Neukum, G., 2008. The lunar and martian cratering records and chronologies. Lunar Planet. Sci. XXXIX. Abstract 2509.
Oehler, D.Z., Allen, C.C., 2009. Mud volcanoes in the martian lowlands: Potential windows to fluid-rich samples from depth. Lunar Planet. Sci. XXXX. Abstract 1034.
Parker, T.J., Saunders, R.S., Schneegerger, D.M., 1989. Transitional morphology in west Deuteronilus Mensae, Mars: Implications for modification of the lowland/upland boundary. Icarus 82, 111–135.
Parker, T.J., Gorsline, D.S., Saunders, R.S., Pieri, D.C., Schneeberger, D.M., 1993. Coastal geomorphology of the martian Northern Plains. J. Geophys. Res. 98, 11061–11078.
Pellenbarg, R.E., Max, M.D., Clifford, S.M., 2003. Methane and carbon dioxide hydrates on Mars: Potential origins, distribution, detection, and implications for future in situ resource utilization. J. Geophys. Res. 108 (E4), 8042. doi:10.1029/2002JE001901.
Potter, P.E., Maynard, J.B., Depetris, P.J., 2005. Mud and Mudstones. Introduction and Overview. Springer, New York. 297 p.
Putzig, N.E., Mellon, M.T., 2007. Apparent thermal inertia and the surface heterogeneity of Mars. Icarus 191, 68–94.
Rice Jr., J.W., Edgett, K.S., 1997. Catastrophic flood sediments in Chryse Basin, Mars, and Quincy Basin, Washington: Application of sandar facies model. J. Geophys. Res. 102 (E2), 4185–4200.
Rodríguez, J.A.P., Tanaka, K.L., Kargel, J.S., Dohm, J.M., Kuzmin, R., Fairén, A.G., Sasaki, S., Komatsu, G., Schulze-Makuch, D., Jianguo, Y., 2007. Formation and disruption of aquifers in southwestern Chryse Planitia, Mars. Icarus 191 (2), 545–567.
Rossbacher, L .A., Judson, S., 1981. Ground ice on Mars – Inventory, distribution, and resulting landforms. Icarus 45, 39–59.
Rotto, S.L., Tanaka, K.L., 1995. Geologic/geomorphologic map of the Chryse Planitia region of Mars, 1:5,000,000 scale. U.S. Geological Survey Miscellaneous Investigations Series Map I-2441.
Salvatore, M.R., Mustard, J.F., Wyatt, M.B., Murchie, S.L., Barnouin-Jha, O.S., 2009. Assessing the mineralogy of Acidalia Planitia, Mars, using near-infrared orbital spectroscopy. Lunar Planet. Sci. XXXX. Abstract 2050.
Salvatore, M.R., Mustard, J.F., Wyatt, M.B., Murchie, S.L., 2010. Definitive evidence of Hesperian basalt in Acidalia and Chryse planitiae. J. Geophys. Res. doi:10.1029/2009JE003519, in press.
Schieber, J., 2003. Black shales. In: Middleton, V., Church, M., Mario Coniglio, Hardie, L.A., Longstaffe, F.J. (Eds.), Encyclopedia of Sediments and Sedimentary Rocks. Kluwer Scientific Publishers, pp. 83–85.
Scholte, K.H., Hommels, A., Van der Meer, F.D., Kroonenberg, S.B., Hanssen, R.G., Aliyeva, E., Huseynov, D., Guliev, I., 2003. Preliminary ASTER and InSAR Imagery Combination for Mud Volcano Dynamics, Azerbaijan. In: 3rd EARSel Workshop on Imaging Spectroscopy, Herrsching, 13–16 May, 2003.
Scott, D.H., Underwood Jr., J.R., 1991. Mottled terrain – A continuing martian enigma. Proc. Lunar Sci. Conf. 21, 627–634.
Scott, D.H., Rice Jr., J.W., Dohm, J.M., 1991. Martian paleolakes and waterways: Exobiologic implications. Origin Life Evol. Biosp. 21, 189–198.
Scott, D.H., Dohm, J.M., Rice Jr., J.W., 1995. Map of Mars showing channels and possible paleolake basins. U.S. Geological Survey Miscellaneous Investigations Series Map I-2461, scale 1:30,000,000.
Skinner Jr., J.A., Mazzini, A., 2009. Martian mud volcanism: Terrestrial analogs and implications for formational scenarios. Marine Petrol. Geol.. doi:10.1016/j.marpetgeo.2009.02.006.
Skinner Jr., J.A., Tanaka, K.L., 2007. Evidence for and implications of sedimentary diapirism and mud volcanism in the southern Utopia highland–lowland boundary plain, Mars. Icarus 186 (1), 41–59.
Skinner Jr., J.A., Tanaka, K.L., Fergason, R.L., 2008. Evidence for and implications of liquefaction in the Vastitas Borealis Marginal Unit in southern Utopia Planitia, Mars. Lunar Planet. Sci. XXXIX. Abstract 2418.
Stewart, S.A., Davies, R.J., 2006. Structure and emplacement of mud volcano systems in the South Caspian Basin. AAPG Bull. 90 (5), 771–786.
Tanaka, K.L., 1997. Sedimentary history and mass flow structures of Chryse and Acidalia Planitiae, Mars. J. Geophys. Res. 102, 4131–4150.
Tanaka, K.L., 1999. Debris-flow origin for the Simud/Tiu deposit on Mars. J. Geophys. Res. 104 (E4), 8637–8652.
Tanaka, K.L., 2005. Geology and insolation-driven climatic history of Amazonian north polar materials on Mars. Nature 437, 991–994.
Tanaka, K.L., Banerdt, W.B., 2000. The interior lowland plains unit of Mars: Evidence for a possible mud ocean and induced tectonic deformation. Lunar Planet. Sci. XXXI. Abstract 2041.
Tanaka, K.L., Joyal, T., Wenker, A., 2000. The Isidis Plains Unit, Mars: Possible catastrophic origin, tectonic tilting, and sediment loading. Lunar Planet. Sci. XXXI. Abstract 2023.
Tanaka, K.L., Skinner Jr., J.A., Hare, T.M., Joyal, T., Wenker, A., 2003. Resurfacing history of the Northern Plains of Mars based on geologic mapping of Mars

Global Surveyor data. J. Geophys. Res. 108 (E4). GDS 24-1–GDS 24-32. doi:10.1029/2002JE001908.
Tanaka, K.L., Skinner Jr., J.A., Hare, T.M., 2005. Geologic map of the Northern Plains of Mars. Scientific Investigations Map 2888, U.S. Geological Survey.
Tanaka, K.L., Rodríguez, J.A.P., Skinner Jr., J.A., Mourke, M.C., Fortezzo, C.M., Herkenhoff, K.E., Kolb, E.J., Okubo, C.H., 2008. North polar region of Mars: Advances in stratigraphy, structure, and erosional modification. Icarus 196 (2), 318–358.
Tosca, N.J., 2009. Clay mineral assemblages derived from experimental acid–sulfate basaltic weathering. Lunar Planet. Sci. XXXX. Abstract 1543.
Van Rensbergen, P., De Batist, M., Klerkx, J., Hus, R., Poort, J., Vanneste, M., Granin, N., Khlystov, O., Krinitsky, P., 2002. Sublacustrine mud volcanoes and methane seeps caused by dissociation of gas hydrates in Lake Baikal. Geology 30 (7), 631–634.
Ware, P., Ichram, L.O., 2006. The role of mud volcanoes in petroleum systems: Examples from Timor, the South Caspian, and the Caribbean. In: Proceedings of the International Conference on Petroleum Systems of SE Asia and Australasia, 1997, pp. 955–958.
Wohletz, K.H., Sheridan, M.G., 1983. Hydrovolcanic explosions, II. Evolution of basaltic tuff rings and tuff cones. Am. J. Sci. 283, 385–413.
Wyatt, M.B., 2008. Chemical alteration of basalt in the Amazonian: OMEGA, TES, and GRS integrated datasets. In: 2008 Annual Meeting of the Geological Society of America, Abstracts with Programs. Abstract 268-3.
Wyatt, M.B., McSween Jr., H.Y., 2002. Spectral evidence for weathered basalt as an alternative to andesite in the northern lowlands of Mars. Nature 417, 263–266.